ACSNANO

www.acsnano.org

ARTICLE

Reductive Adjuvant Nanosystem for Alleviated Atopic Dermatitis Syndromes

Yichao Lu,[#] Xinyu Shan,[#] Jiaxin Huang,[#] Huanli Zhou, Ying Zhu, Sijie Wang, Zhenyu Luo, Xu Liu, Xuemeng Guo, Yingying Shi, Yilong Hu, Huihui Liu, Junlei Zhang, Ping Huang,* Lihua Luo,* and Jian You*

Cite This: *ACS Nano* 2025, 19, 4195–4212

Read Online

ACCESS | Metrics & More | Article Recommendations | Supporting Information

ABSTRACT: **Atopic dermatitis (AD) is a recurrent and chronic inflammatory skin condition characterized by a high lifetime prevalence and significant impairment of patients' quality of life, primarily due to intense itching and discomfort. However, current pharmacological interventions provide only moderate efficacy and are frequently accompanied by adverse side effects. The immune-pathogenesis of AD involves dysregulation of the Th2 immune response and exacerbation of inflammation related to excessive reactive oxygen species (ROS). Therefore, to address these issues, in this study, we targeted the upstream pathogenesis by designing a pro-Th1 adjuvant nanoemulsion loaded with poly(I:C) and encapsulated with the ROS-scavenger vitamin E, termed PV-NE. PV-NE effectively rebalanced the Th1/Th2 immune response and reduced ROS levels both *in vivo* and *ex vivo*, leading to the restoration of immune balance in AD-affected skin and alleviation of symptoms such as lichenification and erythematous patches. In conclusion, our development of the reductive adjuvant nanosystem PV-NE demonstrates its biocompatibility and efficacy in combating AD progression without the use of immunosuppressant glucocorticoids. This has the potential to significantly impact the design and enhancement of pharmacotherapy in future clinical research aimed at curing AD.**

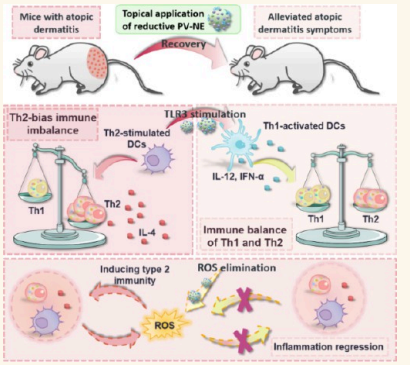

KEYWORDS: *atopic dermatitis, oxidative stress, dendritic cells function modulation, antitype 2 autoimmune inflammation, immune balance restoration*

INTRODUCTION

AD is an autoimmune and heterogeneous skin inflammation that affects over 25% of children and 10% of adults in developed countries. It is characterized by complex pathological features and clinical manifestations, such as recurrent eczematous lesions, including erythematous patches with edema and exudation, crusting, fissuring, and thickening (lichenification). Additionally, AD is accompanied by intense pruritus and impaired epidermal barrier function.[1] Furthermore, AD, which holds a high lifetime prevalence (nearly 33%),[2] can manifest at any point in an individual's life.[3] It may present as either diffuse eczema or localized lesions affecting any skin region,[1] often leading to decreased self-esteem and psychological health disorders in affected individuals. Furthermore, AD is associated with an increased risk of multiple comorbidities, particularly those within the spectrum of atopic disorders. These include, but are not limited to, arthritis, rhinitis, inflammatory bowel disease, and other allergic conditions.[4] In these regards, AD has been gradually identified as the greatest global socio-economic burden among of nonfatal skin conditions.[3] Therefore, given that AD is theoretically controllable and preventable, it would be an indispensable attempt to alleviate AD syndrome in order to maintain the physical and mental health of patients and enhance their quality of life.

Despite the increased prevalence of AD worldwide, especially in developing countries, effective and safe pharmacological interventions for disease control remain elusive. Currently, clinically approved drugs for treating AD, which are characterized by type 2 immune responses, can be broadly categorized into two groups. (1) First is targeted monoclonal antibodies (mAbs) that inhibit key type 2 cytokine signaling pathways, such as interleukin-4 (IL-4) and IL-13. Examples include the anti-IL-4Rα mAb dupilumab and the anti-IL-13Rα mAb tralokinumab.[2] (2) Second is topical or

Received: July 1, 2024
Revised: January 9, 2025
Accepted: January 9, 2025
Published: January 23, 2025

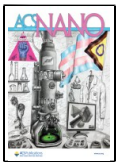

https://doi.org/10.1021/acsnano.4c08767
ACS Nano 2025, 19, 4195–4212

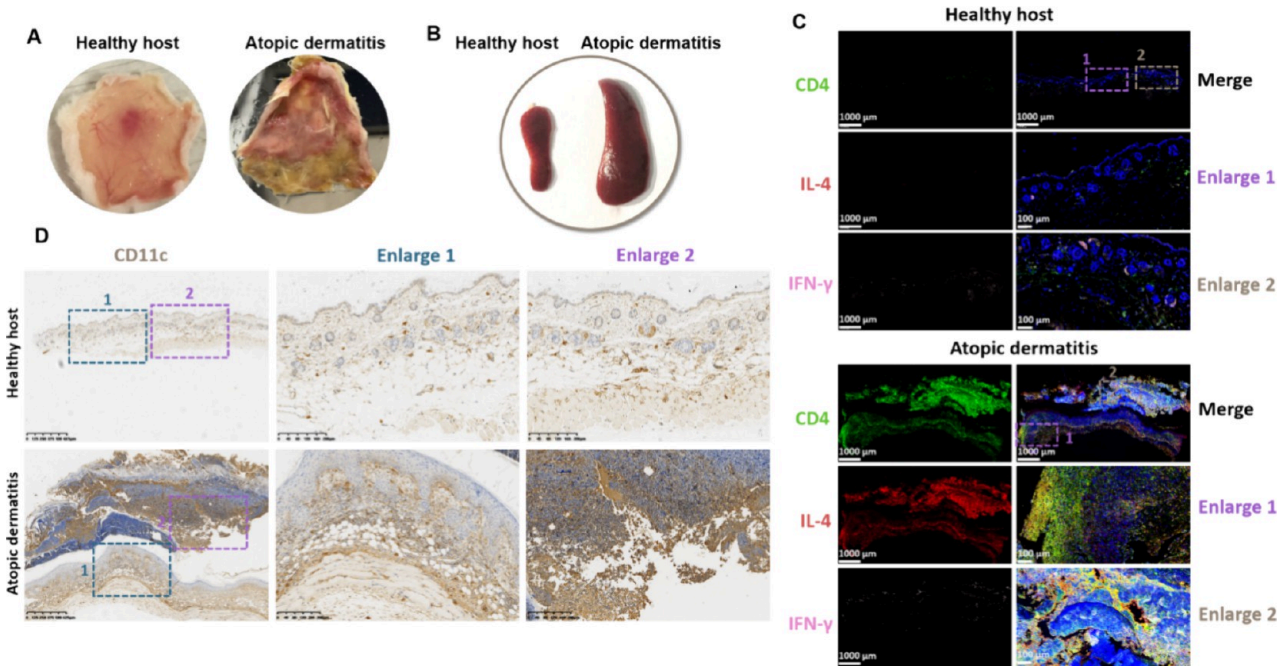

Figure 1. Th2 overwhelming Th1 immune imbalance drives AD. (A) Representative photographs to reflect the skin morphology and (B) the relative spleen size in healthy mouse and the individual with AD. (C) Representative fluorescence images to reflect the infiltration of IL-4$^+$ CD4$^+$ Th2 cells and IFN-γ^+ CD4$^+$ Th1 cells in the skin of healthy or AD mouse. Green: CD4; red: IL-4; pink: IFN-γ; blue: DAPI. Scale bar = 1000 μm and scale bar = 100 μm in enlarged images, respectively. (D) Representative immunohistochemical images to reflect CD11c$^+$ DC infiltration in the skin of the healthy host and the mouse with AD. Scale bar = 625 μm and scale bar = 200 μm in enlarged images, respectively.

systemic immunosuppressants that inhibit both innate and adaptive immune responses. Examples include corticosteroids like dexamethasone and Janus kinase (JAK)-signal transducer and activator of transcription (STAT) inhibitors such as delgocitinib.[1,5] However, the continuous administration of these pharmacotherapies is associated with unavoidable adverse effects. Targeted mAbs, despite their efficacy in mitigating disease severity, pose challenges due to their high cost, limited signaling inhibition for specific pathogenic cytokines, and the potential for disease recurrence after treatment cessation.[6] Moreover, the systemic administration of mAbs may disrupt the immune system in patients with AD.[7] Similarly, immunosuppressants such as corticosteroids present issues including glucocorticoid resistance, topical side effects (such as skin atrophy, withdrawal symptoms, and dermatitis), and systemic adverse effects.[1] Indiscriminate immunosuppression of both innate and adaptive immunity may also lead to localized colonization and opportunistic infections, exacerbating inflammation.[8] Consequently, the expensive and limited mAb therapies,[9] as well as commonly used immunosuppressive strategies, may not be optimal for managing AD. There is an urgent need for treatment options with satisfactory biocompatibility and pharmacologically efficacious in combating AD.

Considering that AD is a skin inflammation closely associated with autoimmunity, its immunopathological mechanisms primarily involve immunological dysregulation within affected areas. Dendritic cells (DCs), which are crucial in initiating both amplified and tolerogenic immunity by selectively driving T helper 1 (Th1), Th2, or regulatory T cell responses, rapidly infiltrate stimulated areas following allergen exposure.[10] They accumulate massively in the inflamed epidermis and dermis, recruiting CD4$^+$ T cells and eliciting robust alloantigen-reactive Th2 immunity, which overwhelms Th1 responses.[2] Subsequently, the excessively developed malgenic Th2 cells locally induce a type 2 proinflammatory cytokine-based immune storm (e.g., IL-4, immunoglobulin E (IgE), and thymic stromal lymphopoietin (TSLP)),[2] promoting the expression of various pruritogens and contributing to AD immunopathology.[3] Hence, given the pivotal role of DCs in orchestrating Th2 responses, manipulating their activation modes and re-establishing the Th1/Th2 balance may represent effective therapeutic strategies. Polyinosinic-polycytidylic acid (poly(I:C)) may be a potent component. Mechanistically, poly(I:C), a synthetic double-stranded RNA (dsRNA),[11] acts as a robust TLR3 agonist, which could induce DCs to adopt a pro-Th1 phenotype[12] and reduce allergen-specific Th2 TL polarization in an inflamed region. This will therefore lead to the shifting effect from AD-eliciting Th2 to Th1 responses and reinstated Th1/Th2 immune balance *in vivo*.

Moreover, excessive ROS exert detrimental effects on the wound healing process and exacerbate localized tissue damage by modulating both physiological and pathological pathways. These pathways include aberrant angiogenesis, improper granulation tissue formation, disrupted extracellular matrix assembly, and sustained inflammation.[13] Additionally, overwhelming ROS-induced oxidative stress synergistically promotes the release of type 2 proinflammatory cytokines (e.g., IL-4), triggers cellular mechanosensitization, and contributes to the formation of the adverse itch-scratch cycle. This cycle further exacerbates epidermal barrier deficiencies and facilitates the colonization of microorganisms.[14] The antioxidant vitamin E possesses potent biological activity, capable of alleviating oxidative stress by scavenging diffusible ROS,[15,16] which may

https://doi.org/10.1021/acsnano.4c08767
ACS Nano 2025, 19, 4195−4212

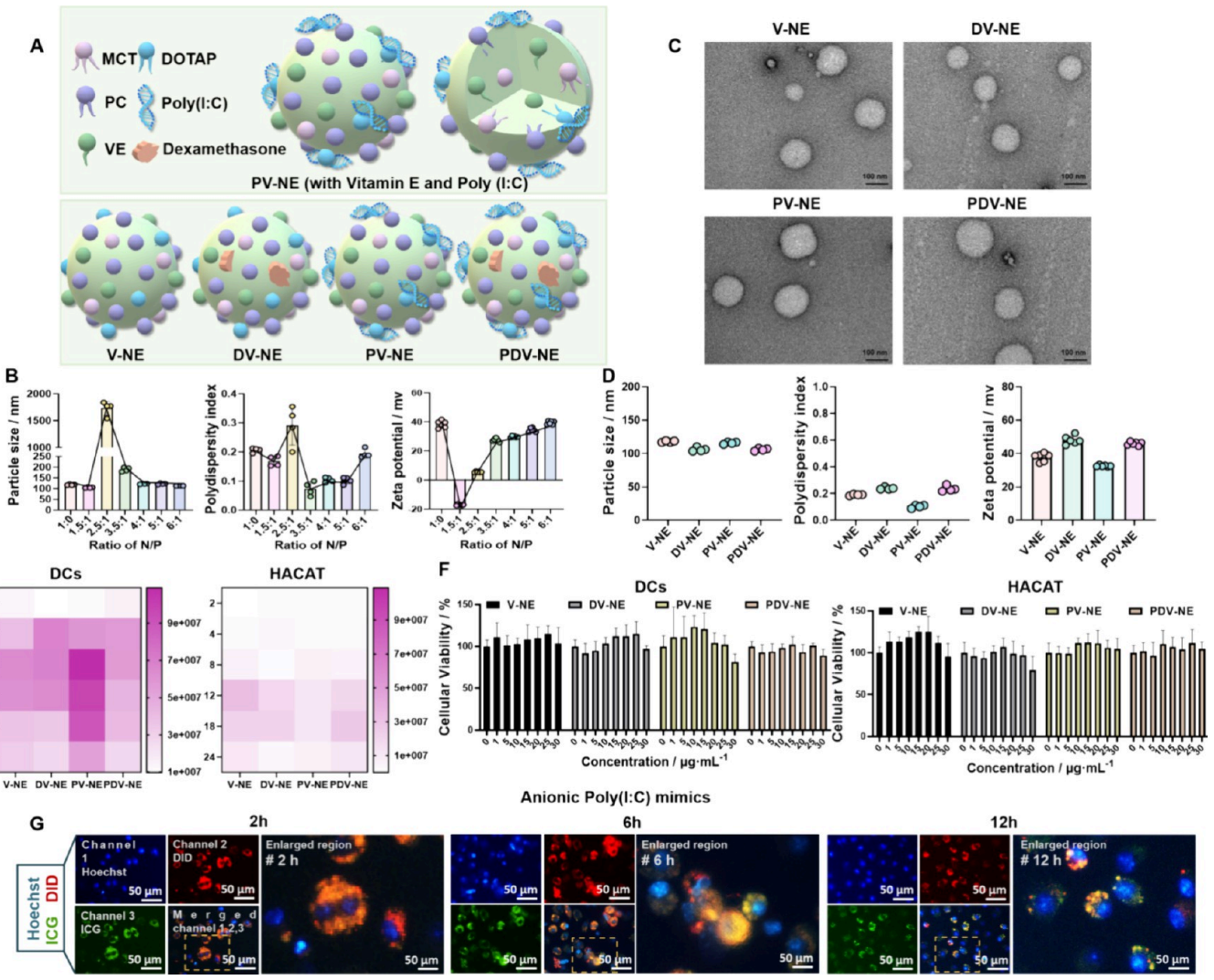

Figure 2. Generation and characterization of PV-NE. (A) Schematic representation of ingredients and three-dimensional structure of four formulations (i.e., V-NE, DV-NE, PV-NE, and PDV-NE). DOTAP, VE: vitamin E, MCT, PC. (B) Particle diameter under dynamic light scattering (n = 4), PDI (n = 4), and surface zeta potential (n = 5) of PV-NE under different ratios of N/P (weight/weight of DOTAP and poly(I:C). (C) Transmission electron microscope (TEM) images to reflect morphologies of nanoscale emulsions (i.e., V-NE, DV-NE, PV-NE, and PDV-NE). Scale bar = 100 nm. (D) Particle size, PDI, and surface charge of the four NEs. (E) Relative quantification of fluorescence intensity to reflect the time-dependent cellular uptake of fluorescent preparations within DCs and HACAT at 2, 4, 8, 12, 18, and 24 h, respectively. (F) Dose-dependent cell viability of indicated cells (i.e., DCs and HACAT) after incubating with NEs (i.e., V-NE, DV-NE, PV-NE, and PDV-NE) at varying drug concentrations for 24 h, respectively. (G) Representative fluorescent images to reflect time-dependent drug-release features of DID- and ICG-labeled PV-NEs in DCs within 12 h. Scale bar = 50 μm. ICG: ICG (green), DID: 1,1′-dioctadecyl-3,3,3′,3′-tetramethylindodicarbocyanine perchlorate (red). All experiments were repeated three times independently, with similar results. All error bars were expressed as ± SD.

contribute to restricting the inflammatory progression and synergistically limiting type 2 immunity.

In these regards, we hypothesize that an effective strategy to alleviate AD syndrome and reduce bacterial colonization involves an upstream pathological pathway-aimed combination approach. This synergistic approach includes (1) regulating the immunological function of DCs to manipulate T helper cell differentiation and promote immune balance restoration in skin lesion foci and (2) inhibiting ROS-based overwhelming oxidative stress to prevent inflammatory exacerbation and further dysfunction of the skin barrier. Here, we set out to construct a biosafe reductive adjuvant nanosystem, termed poly(I:C)-loaded vitamin E nanoemulsion (PV-NE). PV-NE aimed to eliminate excessive ROS and modulate DC function, thereby restoring DC-mediated downstream Th1/Th2 immunological balance and effectively mitigating allergic disorders. Our study highlights the potential of manipulating upstream DC activation modes and immune function to selectively provide a cytokine milieu for diversified T cell development and underscores the crucial connection between reinstating Th2-bias immune deviation and AD syndrome recovery. These findings may offer valuable insights into the design of therapeutic regimens to combat atopic disorders in both preclinical investigations and clinical applications.

RESULTS AND DISCUSSION

Th2-Bias Immune Deviation Triggers AD Progression. Functional cytokines IFN-γ and IL-4 could serve as the marker to distinguish Th1 and Th2, and the two types of cytokines also could further support corresponding Th1 or Th2 lineage

https://doi.org/10.1021/acsnano.4c08767
ACS Nano 2025, 19, 4195−4212

in turn.[17] Besides, previous studies have revealed that recurrent or progressive AD can be triggered by the significant polarization of type 2 cytokine-secreting Th2 cells and Th1/Th2 imbalance in inflamed areas. This imbalance closely correlates with the increased infiltration of pro-Th2 DCs in allergic regions.[1,6,18] Furthermore, ROS-based oxidative stress may perpetuate a mechanical scratching−itching vicious circle and regulate the differentiation of T cells into the Th2 type, thereby potentially exacerbating AD progression.[14]

To evaluate whether dysbiosis in the Th2-prone microenvironment and the accumulation of DCs are crucial contributors to immunopathology in the lesional focus of individuals with AD, we applied 2,4-dinitrochlorobenzene (DNCB) to the naked dorsal skin of mice for 3 consecutive weeks to establish an AD model (Figure S1A). The DNCB-stimulated mice exhibited clinical manifestations resembling those seen in patients with AD. These included skin dryness and crusting in the early stages, followed by flexuous and complex blood vessels, rubefaction, skin barrier integrity impairment, excoriation, thickening (lichenification), erosion, and intense itch at later stages (Figure S1B,C and Figure 1A). Besides, compared to the healthy control, mice with AD displayed significantly enlarged spleens and elevated ROS content (Figure 1B and Figure S1D), indicating an inflammatory reaction akin to that observed in individuals with AD. Furthermore, we observed a significant accumulation of $CD4^+$ IL-4^+ Th2 cells at the DNCB-stimulated site, with minimal infiltration of $CD4^+$ IFN-γ^+ Th1 cells (Figure 1C). This highlights the aberrant immune balance toward the Th2 pathway as a hallmark and a potential pathogenesis of AD.[1] Additionally, considering that DCs are the most multifunctional antigen-presenting cells (APCs) and play a crucial role in T cell trafficking and the activation of diversified T cell populations,[16,19,20] we sought to investigate whether the increased frequency of Th2 cells was consistent with the augmented accumulation of DCs within inflamed lesions. Subsequently, we observed abundant $CD11^+$ DCs deployed in the inflammatory epidermis and dermis foci (Figure 1D and Figure S1E). This suggests that the excessive infiltration of DCs may be associated with the polarization and positioning of the pathogenic Th2 subgroup.

In light of these findings, the Th2-prone immune landscape, characterized by the presence of Th2-recruiting and Th2-stimulated DCs within the lesional microenvironment, coupled with elevated ROS levels, appears to play a crucial role in initiating and exacerbating alloantigen-reactive skin disorder. Therefore, to enhance anti-AD strategies, we propose the following approaches to reinstate the Th1/Th2 immune balance in localized foci: (1) modulating the immune function of DCs to foster diversified differentiation of T cells, thereby gradually shifting the immune response from a Th2-dominant state to a more balanced Th1/Th2 state and (2) eliminating abnormal ROS levels to alleviate oxidative stress. These strategies hold promise for reducing AD symptoms and improving overall treatment outcomes by targeting the underlying immune imbalances and oxidative stress associated with the disease.

Formulation and Characterization of Poly(I:C)-Loaded Vitamin E-Incorporated NE. Considering the positive correlation between overwhelming ROS-triggered oxidative stress and DC-mediated Th2-biased immunological dysregulation in AD development, we fabricated a reductive adjuvant nanosystem named PV-NE (Figure 2A). This NE comprises phosphatidylcholine (PC), medium chain triglyceride (MCT), 1,2-dioleoyl-3-trimethylammoniumpropane (DOTAP), vitamin E, and the TLR3 activator poly(I:C). PV-NE was prepared through facile emulsification, probe sonication, and electrostatic adsorption. In detail, the antioxidant vitamin E scavenges inflammatory ROS, while hydrophobic MCT serves as the core lipid of NEs. Amphipathic PC acts as the surfactant to promote nanoscale construction and structure maintenance, while cationic DOTAP provides a positive charge for anionic poly(I:C) adsorption as well anionic cell membrane for better cellular affinity, stimulating the generation of DCs with pro-Th1 phenotypes. Additionally, considering the common use of local immunosuppressive corticosteroids in alleviating AD symptoms,[1] we formulated three control preparations: dexamethasone-encapsulated NE (DV-NE), poly(I:C)-adhered DV-NE (PDV-NE), and V-NE, which also contain vitamin E (Figure 2A).

Post series of formulation optimization tests of N/P ratio (DOTAP/poly(I:C), weight/weight), PV-NE achieved complete adsorption of the dsRNA analogue poly(I:C) and featured a particle size of 100−150 nm, appropriate polydispersity index (PDI), and cationic zeta potential (around 30 mV) at the N/P ratio of 4:1 (Figure 2B). The NPs could maintain relative stabilization in particle size and zeta potential for at least 18 days at 4 °C (Figure S2A−C). Transmission electron microscopy (TEM) analysis revealed typical spherical structures with a diameter of 100−150 nm (Figure 2C), consistent with dynamic light scattering measurements (Figure 2D). To assess cellular uptake, the fluorescent probe DID was used to label the four NEs (V-NE, DV-NE, PV-NE, and PDV-NE) in Malpighian cell HACAT and DCs. Both cell types efficiently internalized the fluorescent nanoscale emulsions within 24 h, which may be associated with the cell membrane-like lipid component of NEs, slight positive charge in NE surfaces, and the appropriate NE size for cellular internalization. Interestingly, DCs exhibited a more proficient capacity for formulation phagocytosis and internalization compared to HACAT cells, likely due to their inherent APC characteristics (Figure 2E and Figure S2D). Furthermore, cytotoxicity assessment of the formulations in DCs and HACAT cells within 24 h revealed negligible toxicity, with over 80% cell viability for all NEs (Figure 2F), which indicated promising topical application biocompatibility for AD treatments.

To estimate the intracellular drug-release dynamics, we utilized hydrophilic dye indocyanine green (ICG, green) as a model for water-soluble, surface-adsorbed compounds (i.e., poly(I:C)) and oil-soluble dye DID (red) to label the NEs. The absence of complete colocalization between the green fluorescence (ICG) and the red fluorescence (DID) within DCs indicated the release of the surface-adsorbed drug from captured PV-NEs. Interestingly, we observed a progressive release of the adsorptive anionic poly(I:C) mimics from NEs between 6 and 12 h (Figure 2G). Additionally, the intracellular release dynamics of oil-soluble constituents encapsulated within the NEs were assessed using fat-soluble DIO (green) as a mimic for hydrophobic cargos such as dexamethasone and vitamin E, along with DID (red) to mark the formulations. Compared to the electrostatically adhered drugs, the encapsulated cargos exhibited a slower release profile, with partial release occurring after 12 h of coculturing the fluorescent NEs with DCs (Figure S2E).

https://doi.org/10.1021/acsnano.4c08767
ACS Nano 2025, 19, 4195−4212

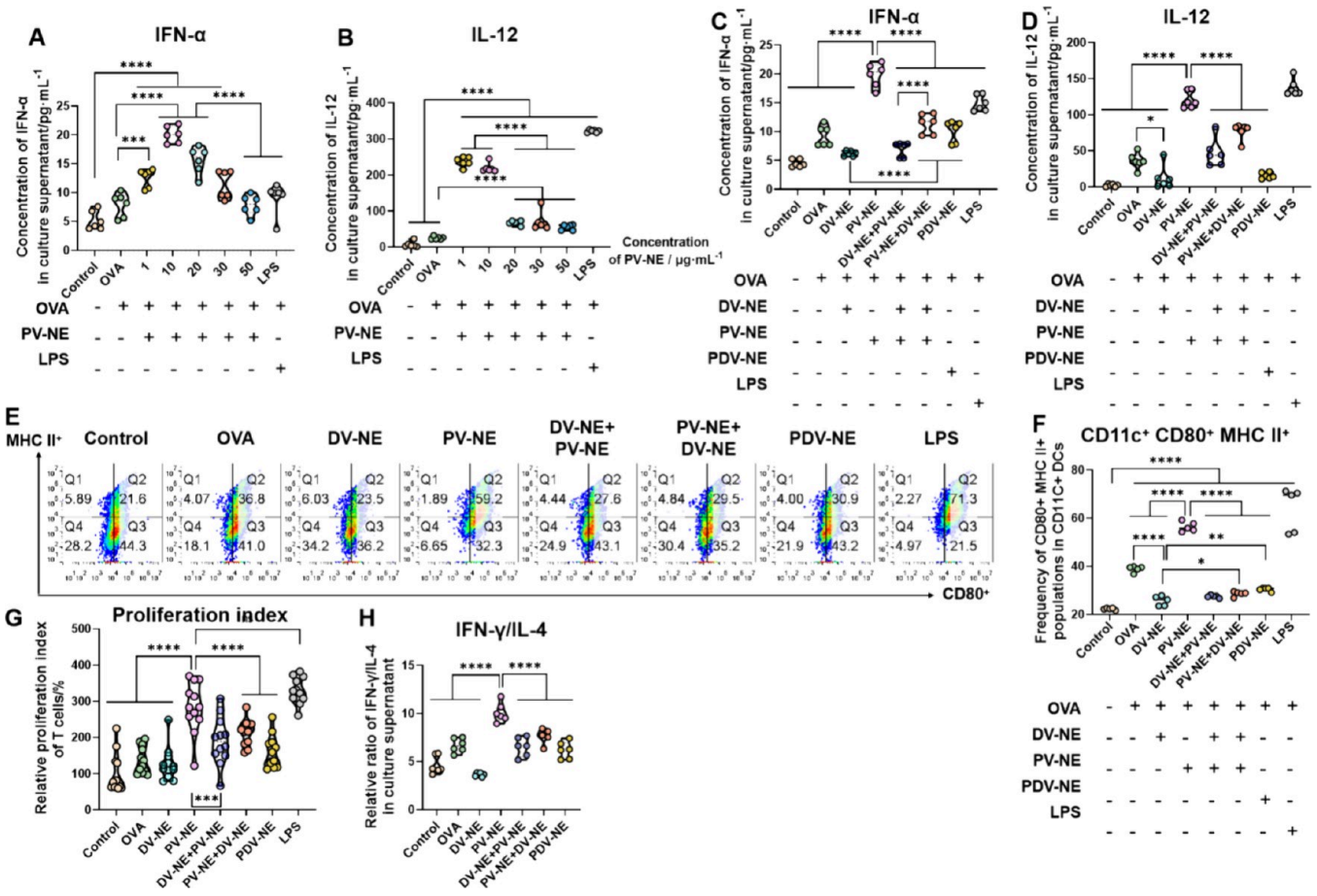

Figure 3. PV-NE endows DCs with Th1-activation immunological competence. (A) IFN-α level and (B) IL-12 concentration in culture supernatant after DCs were treated by different doses (referred to the equivalent concentration of poly(I:C)) of PV-NE and antigen OVA for 24 h. n = 6. (C) IFN-α level and (D) IL-12 concentration in culture supernatant after DCs were cultured with indicated NEs (or LPS) with OVA for 24 h. n = 6. (E) Representative flow cytometric images and (F) summary plot of data to display the frequency of MHC II$^+$ CD80$^+$ cells (pro-Th1 phenotype) in CD11c$^+$ DCs with different treatments. (G) Relative proliferation index of T cells primed by DCs (with different treatments) for 72 h (DCs: T cells = 1:20). n = 12. (H) Relative radioactivity of secreted IFN-γ/IL-4 in the culture supernatant. n = 6. All error bars were expressed as ± SD, *p < 0.05, **p < 0.01, ***p < 0.005, ****p < 0.001.

PV-NE Manipulates DCs into Pro-Th1 Phenotype. DCs, recognized as the most versatile APCs, play a pivotal role in initiating and sustaining immune responses. They can either amplify immune responses against harmful antigen invasion or induce tolerogenic immunity for homeostasis maintenance by providing diverse microenvironment cues for driving various modes of T cell development, such as Th1, Th2, and regulatory T cells (Treg).[16,21] The dosage of antigens and the intensity of costimulation by adjuvants are crucial regulators that modulate DCs' immunological capacity. They influence the functional cytokine secretion, costimulatory molecule expression, and peptide-major histocompatibility complex (p-MHC) expression of DCs.[22] Under a fixed antigen concentration, adjuvants, serving as exogenous analogues of "danger signals" (such as damaged cell-associated molecular patterns (DAMPs) and pathogen-associated molecular patterns (PAMPs)), are essential components exerting immunomodulatory effects by acting on diverse pattern recognition receptors (PRRs) of DCs. This modulation generates different DC phenotypes (e.g., pro-Th1, pro-Th2, and pro-Treg DCs) and regulates the magnitude and durability of DC-based T cell-mediated immunity.[19]

Mechanistically, strongly agonistic ligands of PRRs such as toll-like receptors (TLRs), NOD-like receptors (NLRs), and RIG-like helicases (RLHs) empower DCs with potent cytokine generation capabilities including IL-12 and type I interferon (IFN). They also significantly increase the expression of costimulatory molecules (e.g., CD80 and CD86) and elevate the expression of p-MHC I and p-MHC II, crucial for steering the immune response toward Th1 immunity, characterized by IFN-γ production, through stimulation of T cell receptor (TCR) and cytokine receptor signaling.[19,23] TLR agonists, commonly used vaccine adjuvants, with poly(I:C) being the most potent inducer of type I IFN, are widely combined with other immunotherapies against malignancy development, promoting Th1 immunity.[19,24] Conversely, weaker adjuvant signaling tends to foster Th2 cell (IL-4-producing) or regulatory T cell (IL-10- and TGF-β-generating) immune responses,[25] although the specific mechanisms remain largely unexplored.[22] It is noteworthy that in AD foci, factors derived from Malpighian cells (e.g., TSLP) can skew DC maturation toward Th2-type inflammation.[1,23] In summary, adjuvant-dependent events, under confirmed antigen type and concentration, act as crucial upstream regulators in manipulating DC-based T cell differentiation by influencing downstream TCR signaling duration and intensity on cognate T cells.[22,25] Compared to clinical monoclonal antibody therapy targeting type 2 cytokine production by Th2 cells (e.g., IL-4), using

https://doi.org/10.1021/acsnano.4c08767
ACS Nano 2025, 19, 4195−4212

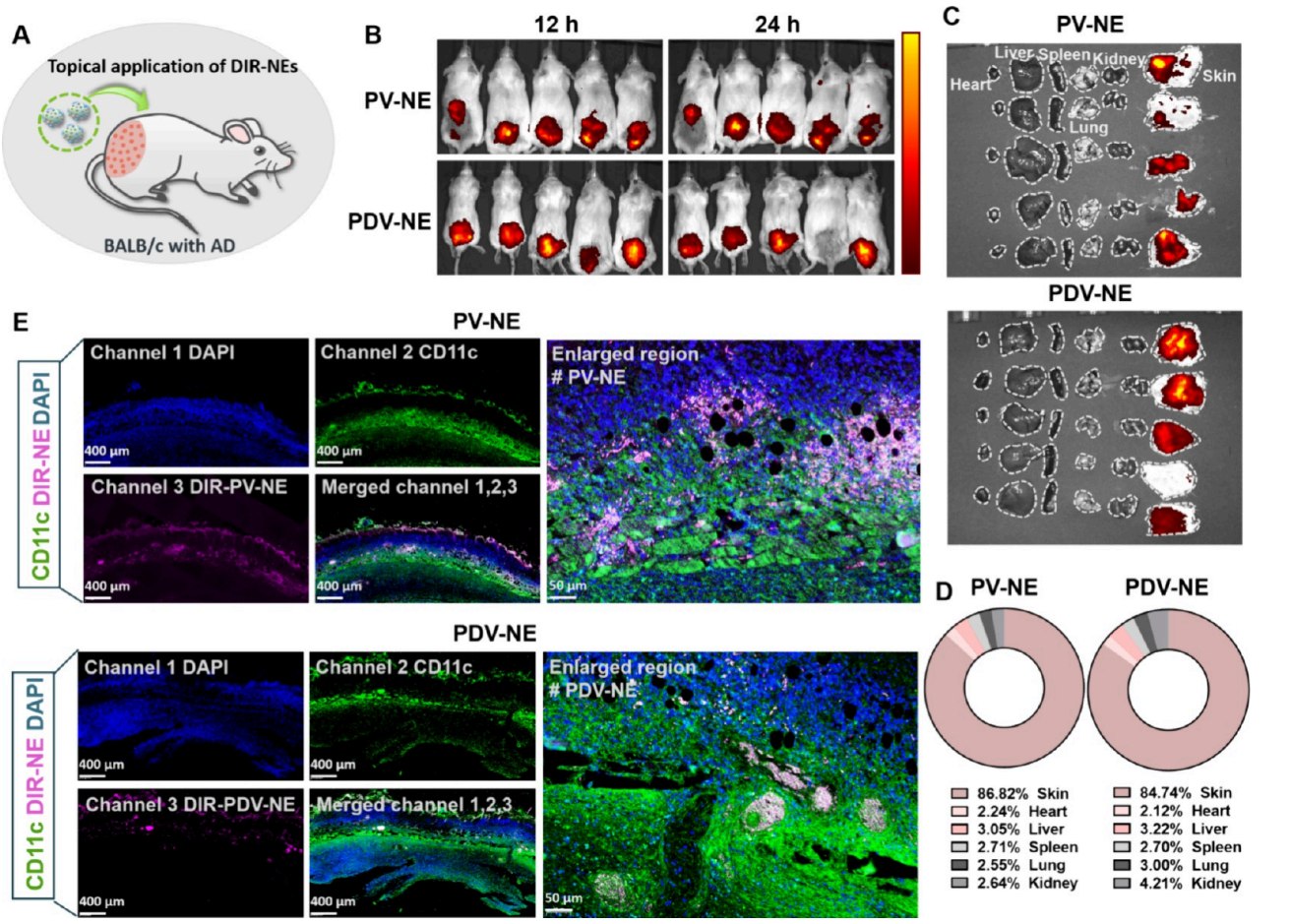

Figure 4. The retention and skin penetration of PV-NE in mice with AD *in vivo*. (A) Diagrammatic sketch of topically administrated NEs in mice with AD. (B) Biodistribution of DiR-labeled PV-NE and PDV-NE at 12 and 24 h post indicated administration (n = 5). (C) Biodistribution and (D) relative fluorescence intensity efficiency indexes (percentage) of DIR-marked NEs (i.e., PV-NE and PDV-NE, respectively) in the heart, liver, spleen, lung, kidney, and skin of AD-bearing mice, after NEs topically applied for 24 h. (E) Representative immunofluorescence images to reflect the skin retention and penetration efficiency as well as colocalization with CD11c$^+$ DCs within the AD lesion foci. DAPI: blue; DIR-NE: pink; CD11c: green. Scale bar = 400 μm and scale bar = 50 μm in enlarged images.

adjuvants to regulate DCs' immunological abilities represents the most upstream event to decrease Th2 polarization and reshape a balanced Th1/Th2 microenvironment.

To assess whether PV-NE can impart DCs with Th1-initiation competence, we initially cocultured DCs with ovalbumin (OVA) antigen (1 mg/mL) along with varying doses of PV-NE or model adjuvant lipopolysaccharide (LPS, a TLR4 activator, 100 ng/mL) for 24 h. Subsequently, we measured the levels of pro-Th1 cytokines (IFN-α and IL-12). Interestingly, we observed a dose-dependent increase in IFN-α and IL-12 secretion with PV-NE treatment, suggesting that 10 μg/mL PV-NE (equivalent to the concentration of poly(I:C)) effectively induced IFN-α and IL-12 production in DCs under fixed antigen concentration (Figure 3A,B). Furthermore, compared to free poly(I:C), PV-NE with surface-adsorbed poly(I:C) demonstrated enhanced effectiveness in endowing DCs with a Th1-initiation phenotype (Figure S3A–D), likely due to the improved stabilization of the dsRNA analogue poly(I:C) after adsorption by cationic NEs.

Additionally, corticosteroids like dexamethasone are commonly used as immunosuppressants to inhibit immune responses mediated by DCs and T cells, thereby alleviating inflammatory disorders. They achieve this by promoting the generation of tolerogenic DCs with a low maturation phenotype, characterized by the reduced expression of p-MHC and costimulatory molecules, as well as a decreased production of IL-12 and type I IFN. However, corticosteroid use may elevate the risk of pathogen-based infections (e.g., fungi and bacteria)[26] and other side effects.[27] To evaluate the immunomodulatory effects of various NEs (i.e., PV-NE, DV-NE, PV-NE combined with DV-NE, DV-NE combined with PV-NE, and PDV-NE) on DCs, we treated DCs with these NEs for 24 h. PV-NE effectively induced the development of Th1-initiating DCs, as evidenced by significantly increased IFN-α and IL-12 production in the culture medium supernatant (Figure 3C,D) and a notable enrichment of MHC II$^+$ CD80$^+$ cells among CD11c$^+$ DCs (Figure 3E,F). In contrast, dexamethasone-encapsulated NEs, particularly DV-NE, inhibited DC maturation. Interestingly, under the current poly(I:C) dosage, combining the immune-activating component poly(I:C) with dexamethasone did not reverse the immature state of DCs induced by dexamethasone, whether poly(I:C) and dexamethasone were incorporated into different formulations and used sequentially or encapsulated in the same NEs (Figure 3C–F). In summary, PV-NE holds promise for generating DCs with a Th1-inducing function, while treatment strategies involving dexamethasone components appear to promote the development of semimature or immature DCs.

https://doi.org/10.1021/acsnano.4c08767
ACS Nano 2025, 19, 4195–4212

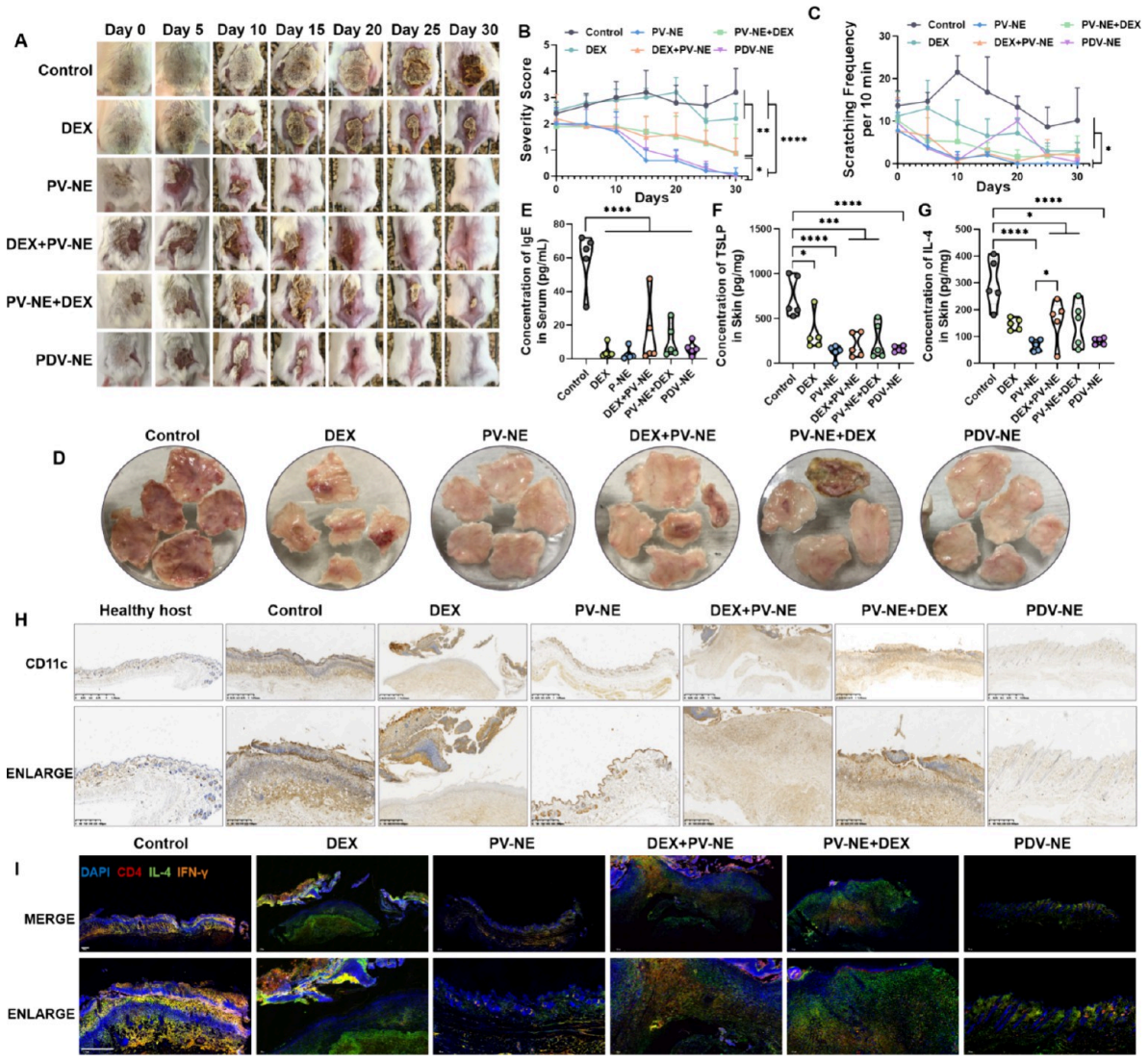

Figure 5. PV-NE effectively alleviates AD symptoms. (A) Representative digital images and (B) severity score curve of mice to reflect the severity/recovery of AD-bearing hosts that were topically applied with different formulations. (C) Scratching frequency of AD-bearing mice within 10 min. (D) Representative digital photographs of dorsal skin in AD lesions. (E) Serum IgE, (F) skin TSLP, and (G) skin IL-4 concentrations as detected by commercial reagent kits (n = 5). (H) Representative immunohistochemical images to reflect CD11c$^+$ DC infiltration within the AD sites after treatment by indicated strategies. Scale bar = 1.25 mm and scale bar = 400 μm in enlarged images. (I) The immunofluorescence images reflect the relative amount of inflammation-infiltrating CD4$^+$ IL-4$^+$ Th2 and CD4$^+$ IFN-γ^+ Th1 within the DNCB-stimulated skin regions after the mice received different treatments. Scale bar = 500 μm and scale bar = 200 μm in enlarged images. DAPI: blue; CD4: red; IL-4: green; IFN-γ: orange. Statistical significance was evaluated by an unpaired two-tailed t test. All error bars were expressed as ± SD, ns = no significance; *p < 0.05, **p < 0.01, ***p < 0.005, ****p < 0.001.

As previously described, DCs capable of producing IL-12 and/or type I IFN (IFN-α) are crucial for promoting IFN-γ^+ Th1 proliferation and initiation during interactions with cognate T cells, while DCs with pro-Th2 competence favor the generation of IL-4$^+$ Th2 cells (Figure S4). To evaluate whether PV-NE-stimulated DCs can influence Th1 differentiation *in vitro*, we coincubated DCs pretreated with the indicated/combined nanoscale emulsions with T cells at a 1:20 ratio for 72 h. Our results showed that PV-NE-stimulated DCs significantly enhanced T cell expansion (Figure 3G) and elicited an IFN-γ^+ Th1 immune response (Figure S5A), while minimizing IL-4$^+$ Th2 induction (Figure S5B). Consistently, PV-NE exhibited a notable immunomodulatory effect and positively altered the DC-based relative ratio of Th1/Th2 *ex vivo* (Figure 3H), prompting further investigation into whether PV-NE can regulate Th1/Th2 responses *in vivo* and restore immunological balance within the Th2-skewed immune landscape in AD lesions.

PV-NE Possesses Favorable Skin Retention and Penetration in AD Foci. Emboldened by our findings demonstrating the enhancement of pro-Th1 immunological competence in DCs (Figure 3C−F) and the manipulation of the Th1/Th2 ratio *in vitro* (Figure 3H), we aimed to assess the skin retention and penetration potential of topically applied PV-NE in inflamed lesions with dysfunctional epidermal barriers in AD-bearing mice (Figure 4A). To facilitate *in vivo* tracking, oil-soluble fluorescent dye DIR was used to label NEs (PV-NE and PDV-NE) for subsequent anti-AD treatment. In brief, to establish the AD mouse model, 1% DNCB solution was applied to the dorsal skin every 2 days for 1 week, followed by stimulation with 0.5% DNCB solution twice per week for another week. Subsequently, fluorescent DIR-labeled NEs were

https://doi.org/10.1021/acsnano.4c08767
ACS Nano 2025, 19, 4195−4212

topically administered to the inflamed AD foci, and their skin retention, permeation efficiency, and biodistribution in the skin and major visceral organs were assessed 24 h postadministration. NEs composed of multiple lipid components exhibited favorable retention within the skin, with the majority reserved in the skin and a minor portion distributed to other visceral organs (Figure 4B−D). Immunofluorescence analysis revealed that both DIR-marked PV-NE and PDV-NE effectively remained on the skin surface and penetrated the impaired barrier to accumulate in deeper skin regions, likely due to the compromised function and impairment of the skin barrier in inflamed AD sites (Figure 4E). Moreover, the penetrated NEs colocalized with infiltrated $CD11c^+$ DCs within the AD lesion focus, suggesting that poly(I:C)-loaded vitamin E-incorporated NEs could be internalized by malgenic DCs and regulate their immunological function to modulate Th1 differentiation and alter the imbalanced Th1/Th2 ratio in AD foci.

PV-NE Effectually Alleviates the Severity of AD Symptoms. Skin, the body's largest protective organ, serves as a barrier against external agents such as bacteria, fungi, toxins, mites, and parasites, utilizing both the stratum corneum barrier and innate and adaptive immunity mechanisms to eliminate harmful microorganisms.[28] Under normal conditions, type 2 immune responses play a protective role by inducing scratching to remove mites and toxins. However, in AD initiation, pathological Th2-biased inflammation (IL-4, IgE, TSLP) leads to uncomfortable scratching behavior and barrier dysfunction (due to impaired keratinocyte terminal differentiation), facilitating increased penetration of cutaneous antigens and microbial colonization, particularly by *Staphylococcus aureus*.[28] Thus, regulating the Th1/Th2 ratio mediated by DCs may help disrupt the type 2 inflammation loop and restore immunological homeostasis in the skin microenvironment.

To assess the potential efficacy of our nanoscale emulsions in addressing inflammatory skin disorders, we utilized a BALB/c mouse model of AD induced by DNCB. This model involved smearing a 1% DNCB solution (in a mixture of acetone and olive oil, at a ratio of 2:1, v/v) for 1 week followed by stimulation with a 0.5% DNCB solution for 2 weeks (Figure S6A). The DNCB-induced AD mice were randomly assigned to various treatment groups, including topical application of dexamethasone cream (DEX), PV-NE, DEX followed by PV-NE, PV-NE followed by DEX, and PDV-NE, administered once daily for 30 consecutive days (Figure S6A). It is important to note that mice receiving DEX plus PV-NE or PV-NE plus DEX were first treated with either DEX or PV-NE and then treated with the other formulation 6 h later. The severity of dermatitis was assessed using a standardized scoring system (0: no symptoms; 0.5−1: mild; 1.5−2.5: moderate; 3−3.5: severe; 4−5: extremely severe) based on AD signs and symptoms, including dryness, excoriation/erosion, erythema/hemorrhage, scratch, and lichenification.[29]

At the termination of the anti-inflammatory experiment, PV-NE with high biosafety and biocompatibility (Figure 2F and Figure S7A) demonstrated effectiveness in alleviating AD symptoms compared with other therapeutic formulations, including the commercial DEX cream. This was evident from the improved AD symptoms observed in digital images, such as reduced lichenification, fissuring, inflamed skin region, and excoriation (Figure 5A), as well as the decreased severity score of AD (Figure 5B and Figure S6B) and scratching behavior (Figure 5C). Moreover, after 1 month of treatment with PV-NE, the mice exhibited hair regrowth in the dorsal region (Figure 5A) and showed relatively normalized skin structure, improved microvasculature, and reduced skin inflammation as well as normalized vascular plexus (Figure 5D). Interestingly, mice treated with DEX cream (DEX group, DEX plus PV-NE, and PV-NE plus DEX) appeared to have suboptimal efficacy in resolving thickened lichenification (Figure 5A). Additionally, both the DEX-treated AD-bearing mice and untreated AD-bearing mice showed massive infiltration of lymphocytes within the liver (Figure S7B), possibly due to prolonged atopic inflammation or DEX-induced hepatitis.

IL-4, a prototypical Th2 cytokine, and TSLP, produced by both Th2 cells and keratinocytes, are considered key contributors to the intense itching experienced by individuals with AD. They activate IL-4Rα[30] and TSLPR,[31] respectively, on sensory neurons, leading to pruritus in AD-suffering murine and humans. This itching can exacerbate AD progression through scratching behaviors. Therefore, reducing local IL-4 and TSLP concentrations may alleviate scratching-related AD severity. Additionally, the transformation of immunoglobulins into IgE is a hallmark of AD progression. Hence, we assessed serum IgE levels and IL-4 and TSLP concentrations in mice skin. Compared to the untreated control, all treatments (including DEX, PV-NE, DEX plus PV-NE, PV-NE plus DEX, and PDV-NE, particularly PV-NE) significantly reduced the levels of these biomarkers (Figure 5E−G).

On the other hand, we also considered the possibility that PV-NE, as a potent pro-Th1 immunomodulator, might induce Th1-skewed hyperimmune responses mediated by DCs in the skin, potentially converting the chronic AD immune microenvironment into an acute type characterized by an IFN-γ-based inflammation. To prevent such Th1-skewed hyperimmunity, we combined PV-NE with DEX cream. Fortunately, mice treated with PV-NE showed a level of $CD11c^+$ DC infiltration in the skin similar to that of healthy mice (Figure 5H and Figure S8). Impressively, immunofluorescence results suggested that the topical application of PV-NE did not induce an IFN-γ storm and could restore Th1/Th2 homeostasis in the skin (Figure 5I).

PV-NE Effectively Mitigates the Severity of AD Symptoms under Recurrent Attacks. Given that atopic disorder is clinically characterized by recurrent eczematous lesions triggered by allergens or other allergic agents,[1] we aimed to assess the effectiveness of PV-NE in alleviating AD symptom severity under repeated exposure to the pro-Th2 immunity stimulator DNCB. After prestimulating the mice with a 1% DNCB solution three times within 1 week, we randomly assigned them to different treatment groups. These groups received topical applications of various formulations, including commercial DEX cream, PV-NE, DEX plus PV-NE, PV-NE plus DEX, and PDV-NE, on the inflamed dorsal skin every day for 3 consecutive weeks, while continuing to apply 0.5% DNCB throughout the treatment period (Figure S9A).

Interestingly, the progression of AD under recurrent attacks appeared to differ from the results of the *in vivo* anti-AD experiment described in PV-NE Effectually Alleviates the Severity of AD Symptoms. Throughout the continuous DNCB stimulation period, the severity of AD symptoms worsened due to the potent induction of pro-Th2 immune responses by the allergens despite the consecutive application of respective treatments to the AD-bearing mice. Although the untreated mice consistently experienced disease exacerbation with repeated exposure to allergic agents, the mice topically treated

https://doi.org/10.1021/acsnano.4c08767
ACS Nano 2025, 19, 4195−4212

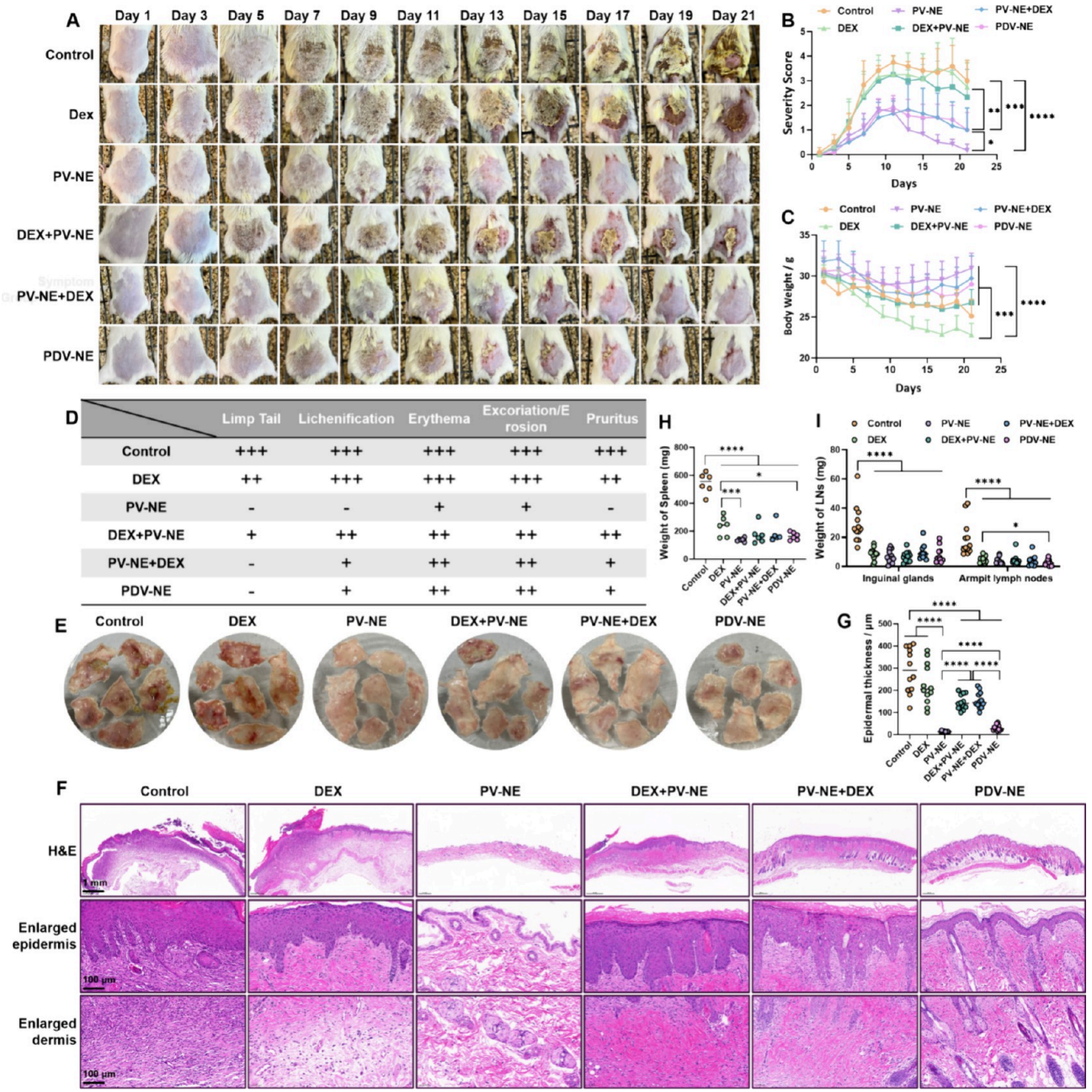

Figure 6. Topical application of PV-NE attenuates the severity of recurrent AD attacks. (A) Representative digital images, (B) severity score curve, and (C) body weight of mice to reflect the severity/recovery of AD-bearing mice that were topically administrated with indicated formulations. (D) AD symptoms to reflect the severity and (E) representative digital images of the dorsal skin at the termination of the experiment. (F) Representative H&E staining photographs to reflect the structure and thickness of skin with AD lesion after treatment. Scale bar = 1 mm and scale bar = 100 μm in enlarged images. (G) Quantification of epidermal thickness in the skin with an AD lesion after treatment. (H) Quantitative weight of the spleen and (I) inguinal and infra-axillary lymph nodes (LNs) from the mice that accepted the indicated treatments. Statistical significance was evaluated by an unpaired two-tailed *t* test. All error bars were expressed as ± SD, ns = no significance; *$p < 0.05$, **$p < 0.01$, ***$p < 0.005$, ****$p < 0.001$.

with PV-NE gradually exhibited satisfactory recovery from this stubborn disease, to some extent (Figure 6A,B and Figure 9B). Moreover, compared to the significant decrease in body weight observed in the mice treated with commercial DEX cream and the untreated control group, the PV-NE-treated mice maintained an almost stable body weight (Figure 6C), indicating the biosafety of PV-NE (Figure S10A) and its ability to control dermatitis progression or maintain a healthy condition. Furthermore, at the end of the experiment, we assessed the overall health condition and AD symptoms of the mice before their sacrifice. We observed that PV-NE-treated mice showed strong tails, reduced lichenification, alleviated pruritus, relatively improved erythema, and very mild excoriation/erosion, as shown in (Figure 6D). Additionally, PV-NE was able to alleviate inflammatory skin symptoms (e.g., flexuous complex vascular plexus, rubefaction, and lichenification) (Figure 6E), suggesting that PV-NE effectively facilitated the rehabilitation of AD symptoms under recurrent attacks.

https://doi.org/10.1021/acsnano.4c08767
ACS Nano 2025, 19, 4195−4212

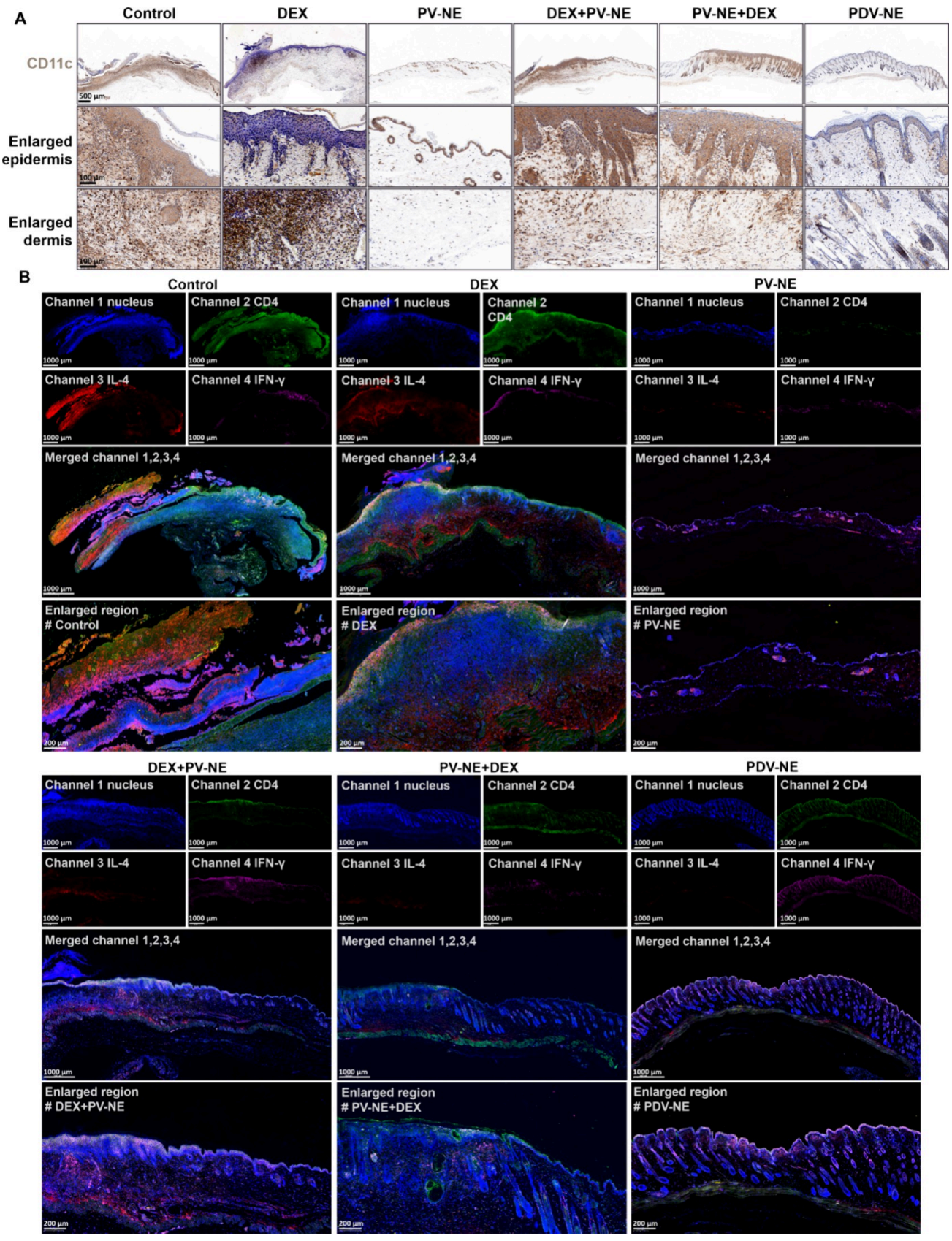

Figure 7. Topical application of PV-NE alters immunological landscape in the lesions under recurrent AD attacks. (A) Representative immunohistochemical images to reflect $CD11c^+$ DC infiltration within the AD sites after treatment by indicated strategies. Scale bar = 500 μm and scale bar = 100 μm in enlarged images. (B) The immunofluorescence images reflect the relative amount of inflammation-infiltrating $CD4^+$ IL-4^+ Th2 and $CD4^+$ IFN-γ^+ Th1 within the iteratively DNCB-stimulated skin sites after the mice accepted different treatments. Scale bar = 1000 μm and scale bar = 200 μm in enlarged images. DAPI: blue; CD4: green; IL-4: red; IFN-γ: pink.

https://doi.org/10.1021/acsnano.4c08767
ACS Nano 2025, 19, 4195−4212

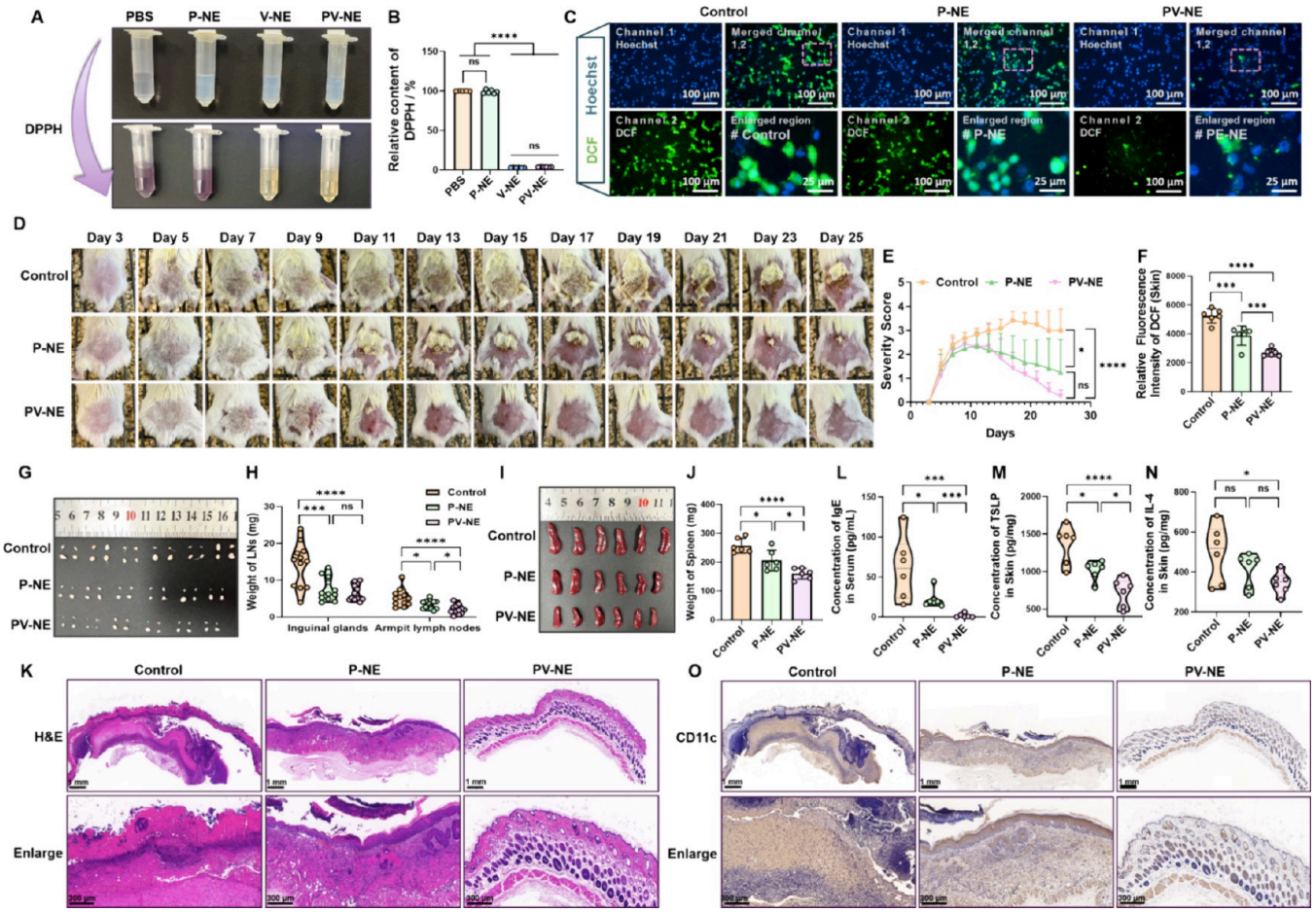

Figure 8. Combination of ROS scavenger and adjuvant nanoplatform elicits synergistically anti-AD effectiveness. (A) Color change of the DPPH solution as well as (B) the relative quantification of DPPH content to appraise the radical scavenging activity of indicated NEs (i.e., P-NE, V-NE, and PV-NE). (C) Representative fluorescent images to reflect the ROS content within the H_2O_2-pretreated human Malpighian cell HACAT after treatment by indicated NEs (i.e., P-NE and PV-NE). Scale bar = 100 μm and scale bar = 25 μm in enlarged images. Green: DCF; Blue: Hoechst. (D) Representative digital images and (E) severity score curve of AD-bearing mice to reflect the AD progression after the mice were topically applied with indicated formulations within 25 days (n = 6 biologically independent animals in each group). (F) Relative content of ROS in the mice's dorsal skin at the termination of the experiment. (G) Images and (H) quantitative weight of the inguinal and infra-axillary lymph glands from the mice that accepted the indicated treatments. (I) Digital photographs and (J) quantification of the spleen from the mice that accepted the indicated treatments. (K) Representative H&E staining photographs to reflect the structure and thickness of the skin with AD lesion after treatment. Scale bar = 1 mm and scale bar = 100 μm in enlarged images. (L) Serum IgE, (M) skin TSLP, and (N) skin IL-4 concentrations as detected by commercial reagent kits (n = 6). (O) Representative immunohistochemical images to reflect $CD11c^+$ DC infiltration within the AD sites after treatment by indicated strategies. Scale bar = 1 mm and scale bar = 100 μm in enlarged images. Statistical significance was evaluated by an unpaired two-tailed t test. All error bars were expressed as ± SD, ns = no significance; *p < 0.05, **p < 0.01, ***p < 0.005, ****p < 0.001.

Moreover, since the thickened epidermis and hypertrophied upper layer are prominent indicators or clinical characteristics in evaluating the progression of AD,[1] the hematoxylin−eosin (H&E) staining analysis was utilized to assess the structure and epidermal thickness of the skin within the inflammatory foci after different treatments. Subsequently, the detailed skin tissue analysis further revealed that the reductive adjuvant-loaded nanoplatform PV-NE, aimed at altering DC-mediated Th1/Th2 differentiation *in situ*, could relatively restore the abnormal structure (Figure 6F) as well as rehabilitate the thickened dermis and epidermis (Figure 6G), compared with the untreated AD-suffering mice. However, the commercial DEX cream seemed to exhibit relatively moderate therapeutic effectiveness in either mitigating the severity of AD symptoms or altering the inflammatory skin structure and dermal/epidermal thickness (Figure 6F), which may be partially due to (1) the immunosuppressant properties of DEX and the consequent opportunistic infection or the promotion of bacterial colonization (e.g., *S. aureus*) and (2) glucocorticoid resistance.

Furthermore, considering that AD is a chronic inflammation featuring prominent secondary lymphoid tissues (SLOs, e.g., lymph node and spleen), we sought to appraise the SLO expansion in the DNCB-induced mice after the indicated therapeutics. We observed that the AD mice accepting treatments (including DEX cream, different NEs, and the combination of NEs and DEX cream) could all alter their spleens' (Figure 6H and Figure S10B) as well as LNs' (Figure 6I and Figure S10C) size and mass compared to the negative control.

PV-NE Reinstates the Balanced Immune Contexture under AD Recurrent Attacks. As previously reported, the localized AD inflammation locus is characterized by disrupted microenvironment homeostasis including aberrant keratino-

https://doi.org/10.1021/acsnano.4c08767
ACS Nano 2025, 19, 4195−4212

cyte terminal differentiation, dysregulated epidermal barrier function, overwhelming ROS production, and immunopathological Th2 immune deviation. Therefore, our goal was to manipulate the generation and activation of Th1 and Th2 cells based on DCs through topical application of the reductive adjuvant nanosystem PV-NE, which may contribute to the restoration of the diverse imbalance or dyshomeostasis within AD sites. Given that we observed PV-NE could restore abnormal dermal/epidermal thickness (Figure 6F) and promote skin barrier rehabilitation (Figure 6A,E), we further explored the immune landscape within the AD lesion microenvironment. We found that inflammation-infiltrating $CD11c^+$ DCs significantly decreased after consecutive PV-NE-based treatment (Figure 7A and Figure S11) which may facilitate the normalization of pro-Th2 DC infiltration-mediated immune dysbiosis and consequently alleviate AD symptoms based on type 2 immunity. Additionally, we detected the levels of type 2 cytokines associated with the initiation and progression of AD through an enzyme-linked immunosorbent assay (ELISA). Impressively, AD indicators such as IgE content in serum (Figure S12A), pro-AD TSLP (Figure S12B), and IL-4 concentration (Figure S12C) within the skin foci were decreased after PV-NE administration, accompanied by low levels of the type 1 cytokine (i.e., IFN-γ) in the skin (Figure S12D).

Subsequently, immunofluorescence was employed to explore the relative frequency of $CD4^+$ IL-4^+ Th2 and $CD4^+$ IFN-γ^+ Th1 cells in the inflammatory region after treatment, which corroborated the cytokine levels obtained from ELISA. The untreated DNCB-induced mice demonstrated overwhelming Th2 immune response or Th2-tipping immune dysregulation and exhibited obvious thickening of the epidermis and dermis. Interestingly, after PV-NE application, the mice exhibited lower inflammation levels with a balanced Th1 and Th2 ratio and possessed thinner dermal/epidermal thickness (Figure 7B), suggesting that the appropriate anti-AD therapeutic effects of PV-NE may be interconnected with the restoration of the imbalanced immune context in recalcitrant inflammatory disorders.

Combined ROS Elimination and Adjuvant-based Modulation Facilitates Synergistic Effectiveness. Excessive ROS within the lesional focus of AD can foster the secretion of proinflammatory cytokines, such as IL-4; provoke an adverse itch−scratch cycle and type 2 immune loop; and further exacerbate the dysregulation of the skin barrier, aggravating AD progression.[14] Therefore, in the anti-AD experiment described above, we adopted an integrated therapeutic strategy to ameliorate AD syndrome by topically applying PV-NE, which encompasses a ROS-eliminating component (vitamin E) and the adjuvant poly(I:C) that can modulate DCs' immune function. This strategy aimed at both (1) manipulating the immune competence of DCs to regulate the relative ratio of Th1/Th2 and contribute to immune balance restoration in skin lesional foci and (2) blocking ROS-based oxidative stress to avoid exacerbated inflammation and synergistically promote the restoration of microenvironment homeostasis. Encouraged by the AD-alleviating effect of PV-NE, we sought to further investigate whether the combination of a ROS-eliminator and DCs-modulator (adjuvant) could potentiate the capacity to mitigate the severity of AD symptoms compared to a single usage of the adjuvant alone.

Therefore, we constructed a poly(I: C)-loaded NE (P-NE, without the radical scavenger vitamin E) to function as a control NE for exploring the synergistic effectiveness of the ROS scavenger and adjuvant component. The P-NE characterized a spherical structure with a diameter around 100−150 nm (Figure S13). Subsequently, DPPH (2,2-diphenyl-1-picrylhydrazyl) was utilized to imitate the ROS radicals. We discovered that both the V-NE and PV-NE possessed a potent capacity to scavenge the radical component, while P-NE did not display any competence to eliminate the ROS within the DPPH solution (Figure 8A,B). Next, we used 300 mM H_2O_2 to pretreat the human Malpighian cell HACAT to estimate the intracellular ROS-scavenging activity of PV-NE. PV-NE-treated HACAT displayed much lower endocellular ROS contents compared with the P-NE-treated and untreated HACAT (Figure 8C), which implied that PV-NE showed reductive properties *in vitro*.

Subsequently, we established an AD mice model with recurrent attacks and tried to explore the synergistic efficacy of combining a reductive composition and DC modulator within 25 days (Figure S14A). Impressively, compared with the negative control, the single usage of adjuvant (i.e., P-VE) did attenuate the severity of AD under repeated stimulation of DNCB (Figure 8D,E and Figures S14B,C) to a certain extent, which may be attributed to the altered ratio of Th1/Th2 *in situ*. However, it was noteworthy that PV-NE possessed optimal AD-alleviating effectiveness, as evidenced by the better-recovered dermatitis symptoms and no decline in body weight (Figure S14D), together with decreased inflammation both in the localized skin lesional region (the reduced ROS content) (Figure S14E and Figure 8F) and in the proinflammatory secondary lymphoid organs (SLOs) (Figure 8G−J). The detailed H&E staining demonstrated that although the reduplicated stimulation of the pro-type 2 reagent DNCB would lead to destructive structural changes in the skin (particularly the almost necrotic horny layer and dysfunctional epidermal barrier), PV-NE treatment could effectively facilitate normalization or homeostasis of the inflamed skin sites (Figure 8K), which may be associated with the massively declined ROS concentration (or relieved oxidative stress) within the AD lesion after the PV-NE-mediated treatment (Figure 8I). Furthermore, the important hallmarks of AD, including the IgE in serum and the TSLP and IL-4 in the skin, all significantly decreased after the mice received treatments (both P-VE and PV-NE) (Figure 8L−N). Impressively, the administration of PV-NE would not significantly augment the IFN-γ-secreting Th1 frequency or induce chronic inflammation into the acute type in the lesion foci (Figure S14F), which could contribute to the inflammation regression and decreased $CD11c^+$ DC infiltration (Figure 8O and Figure S15), as well as maintained homeostasis instead. On the other hand, although P-NE could to some extent promote the amelioration of AD by altering the Th1/Th2 differentiation within the inflamed locus, P-NE without the reductive constituent still demonstrated relatively modest anti-AD pharmacological efficacy compared to PV-NE. This difference in efficacy may be attributed to the fact that the immune landscape of Th1/Th2 was not completely homeostatic or that inflammation caused by ROS was not completely eliminated. Further exploration is still required to understand the intrinsic mechanisms underlying these observations.

In brief, all the results presented herein implied that the topical application of biosafe PV-NE (Figure S16) could promote the recovery of AD symptoms or avoid inflamed AD

https://doi.org/10.1021/acsnano.4c08767
ACS Nano 2025, 19, 4195−4212

progression via facilitating the homeostasis rehab, even if the hosts under repeated stimulation of DNCB.

DISCUSSION

As a chronic autoimmune skin disorder, AD often initiates the atopic march, leading to the development of other conditions such as food allergies, allergic rhinitis, and asthma.[32] Despite available medical treatments, AD remains incurable, particularly in cases of severe or recalcitrant disease.[14] Pathologically, massively accumulated DCs and overwhelmed ROS are important inducers of AD progression. DCs, the most important antigen-presenting cells to orchestrate T cell immunity, massively infiltrate in the inflamed epidermis and dermis of AD lesion, recruit $CD4^+$ T cells, and then boost pathogenic alloantigen-reactive Th2 immunity.[2,3,10] DCs are the upstream manipulators of pathogenic Th2 immunity actually. However, a considerable part of treatments aims at restricting the pathogenic and complexed Th2 immunity,[6,7] and the importance of regulating DCs' immunological competence is ignored. Besides, excessive ROS exacerbates localized tissue impairment by inducing an adverse itch−scratch cycle, leading to epidermal barrier deficiencies, eliciting IL-4 release, supporting aberrant angiogenesis, and maintaining inflammation.[13,14] Therefore, eliminating the overwhelming ROS is beneficial to support AD recovery and regulate the immune environment. However, the importance of extra ROS elimination has not attracted enough attention in immune modulation. In these regards, we constructed a nanoplatform PV-NE that codelivered immunoregulatory adjuvant and reductive ROS scavenger to alleviate the severity of AD symptoms by synergistically functioning on the upstream immunopathology.

On the other hand, common therapies, including glucocorticoids, antihistamines, and anticytokine mAbs, can alleviate symptoms but often come with side effects (e.g., sleep disturbance, cushing syndrome, and glucocorticoid resistance)[33] and economic burdens. To address this challenge, there is a pressing need for alternative therapies to manage AD effectively on a daily basis. In other words, finding optimized treatments with cost-effectiveness together with long-term efficacy and safety may be in urgency, particularly for moderate-to-severe patients in low-income levels.[9] On the one hand, the inexpensive topical corticosteroids is the first-line therapy for mild-to-moderate AD patients, by nonselective anti-inflammation effect.[3] However, the application of topical corticosteroids may suffer from their various adverse reactions (e.g., secondary or aggravated infection, skin atrophy and telangiectasia),[8] relative moderate effectiveness, and glucocorticoid resistance in long-term treatments.[3] Recognizing that dysregulated immune responses involving DCs and the inflammatory itch−scratch cycle contribute significantly to AD pathogenesis, we developed a reductive adjuvant nanoplatform (PV-NE). This innovative approach aims to scavenge excessive ROS while modulating DCs' immune function to rebalance the Th1/Th2 ratio, thereby disrupting the Th2-dominated immune response and breaking the cycle of inflammation and itching. Hence, considering the pathogenesis-targeted strategy and the results in the paper, compared to the nonselective immunosuppressants (represented by DEX), PV-NE may hold better anti-AD outcomes and relative biosafety for moderate-to-severe patients or individuals with recurrent AD attacks. On the other hand, with the increasing understanding of type 2 immunity-based pathogenesis of AD, the biologic treatments (e.g., anti-IL-4Rα mAb dupilumab) gradually occurred recently,[2] which possess more effective outcomes in moderate-to-severe AD patients than traditional topical therapies. However, the effective but more expensive biologic treatments (especially mAb therapy) are likely to lead to higher costs.[34] In this connection, as not involved in a complicated biologic preparing process, PV-NE may be simpler in formulation and possess a relatively low-cost feature. Consequently, PV-NE, with an immune-regulating and ROS-scavenging effect to target the upstream pathogenesis, may serve as a cost-effective, safe, and efficacious candidate to alleviate AD and reduce AD recrudesce.

Concerned about the potential or possibility of PV-NEs to induce a shift from chronic Th2 inflammation to acute Th1 inflammation due to their potent adjuvant poly(I:C) delivery, we took precautions by exploring combination therapies. We investigated combining PV-NE with a commercial DEX cream (PV-NE plus DEX and DEX plus PV-NE) and directly codelivering poly(I:C) and DEX (PDV-NE). Besides, considering the quite long dosing interval between DEX and PV-NE as well as the validated stability of the commercial DEX cream, the stability of DEX cream may not be easily disrupted by the other preparation. Specially, we have conducted a preliminary experiment before the anti-AD experiment *in vivo* and have validated that the successively topical application of DEX and PV-NE would not disrupt the properties of each other, as there was no evident physical change of these formulations. In a word, these combined approaches aimed to modulate the Th1/Th2 ratio through PV-NE while simultaneously inhibiting excessive Th1 expansion and preventing acute inflammation with DEX's anti-inflammatory properties.

Intriguingly, a single application of PV-NE did not lead to localized IFN-γ accumulation in the AD locus but instead contributed to inflammation regression and restored microenvironment homeostasis. This led to mitigated AD symptoms, even under recurrent attacks of DNCB stimulation. While P-NE, lacking the anti-ROS component, could still alter the Th2-tipping immune imbalance and aid in the recovery of recurring AD by promoting Th1 generation, its effectiveness compared to PV-NE was moderate. This may be attributed to the incomplete removal of inflammation caused by ROS or the relative accumulation of IFN-γ, requiring a further exploration of the underlying mechanism.

Indeed, the management of lichenification holds paramount importance in a therapeutic regimen for AD, particularly during recurrent flare-ups. The achievement of normalization or a gentle reduction in lichenification can substantially contribute to the restoration of functional skin integrity and augment the efficacy of anti-AD interventions. However, isolated applications of DEX cream or its combination with the PV-NE nanosystem, particularly in the sequence of DEX cream followed by PV-NE, have demonstrated limited success in mitigating the thickness of lichenified skin. Rather, persistent lichenification, which overlays inflamed skin, may persist in disrupting normal skin architecture and undermine the protective barrier function of the epidermis. Therefore, alternative approaches may be necessary to address this aspect of AD treatment effectively.

In these regards, facilitating the rehab of imbalance of the Th2-tipping immune deviation as well as ROS-dependent inflammation for anti-AD pharmacological interventions may be an important direction in future clinical application.

https://doi.org/10.1021/acsnano.4c08767
ACS Nano 2025, 19, 4195−4212

CONCLUSIONS

Herein, we proposed a therapeutic strategy to alleviate recurrent or recalcitrant AD symptoms by aiming at the upstream pathological pathway for a more efficacious effect. By effectively manipulating the immunological capability of DCs, PV-NE modulates the balance between Th1 and Th2 cells both *in vivo* and *ex vivo*. Furthermore, the codelivery of a ROS scavenger along with the potent adjuvant poly(I:C) within PV-NE exhibits a synergistic anti-AD efficacy. This combination simultaneously eliminates abnormal ROS levels and regulates the exaggerated Th2-skewed immune deviation prevalent within inflamed AD lesions. In summary, this therapeutic approach demonstrates satisfactory biocompatibility and significant clinical potential in combating progressive AD, offering valuable insights into the design and development of therapeutic regimens for AD initiation and progression.

METHODS AND EXPERIMENTAL

Materials and Reagents. Vitamin E, DEX, OVA, LPS, and DNCB (CAS: 97-00-7) were bought from Sigma-Aldrich (Merk, Darmstadt, Germany). Poly(I:C) (CAS: 24939-03-5) was purchased from MedChemExpress (Monmouth Junction, NJ, USA). Phosphatidylcholine PL100M, MCT, and DOTAP were acquired from Kewpie Co. (Shibuya, Japan), Lipoid (Merk, Darmstadt, Germany), and Avanti Co., Ltd. (USA), respectively. IFN-γ, IL-4, and CD11c antibodies were obtained from Proteintech (Chicago, USA). Fat-soluble dyes 1,1′-dioctadecyl-3,3,3′,3′-tetramethylindodicarbocyanine perchlorate (DID, CAS: 127274-91-3), 3,3′-dioctadecyloxacarbocyanine perchlorate (DIO, CAS: 34215-57-1), and 1,1-dioctadecyl-3,3,3,3-tetramethylindotricarbocyaine iodide (DIR, CAS: 100068-60-8) were acquired from Meilun Biotech Co. Ltd. (Dalian, China), and the water-soluble electronegative dye ICG was gained from Tokyo Chemical Industry (Tokyo, Japan). FITC-antimouse CD80, PE-antimouse MHC II (MHC I I-A/I-E), and APC-antimouse CD11c antibodies utilized for flow cytometry were purchased from Biolegend (San Diego, CA, USA). Murine IFN-α and IgE enzyme-linked immunosorbent assay (ELISA) kits were purchased from Jiangsu Meimian Industrial Co., Ltd. (Jiang Su, China). TSLP, IL-4, IFN-γ, and IL-12p40 ELISA kits were gained from MultiSciences (Lianke) Biotech Co., Ltd. (Hang Zhou, China). Cell Counting Kit-8 (CCK-8), the fluorescence-marked 2-deoxy-glucose analogue 2-NBDG (CAS: 186689-07-6), and nuclear dye Hoechst 33342 (CAS: 23491-52-3) were obtained from GLPBIO (USA). Murine recombinant cytokine granulocyte-macrophage colony stimulating factor (GM-CSF), IL-2, IL-4, and IL-7 were purchased from Peprotech (New Jersey, USA). L-Glutamine, nonessential amino acids (NEAAs), RPMI 1640 medium, penicillin/streptomycin (100 U L^{-1}), 0.25% trypsin with 0.02% ethylenediaminetetraacetic acid (EDTA), Dulbecco's modified Eagle medium (DMEM), and sodium pyruvate along with fetal bovine serum (FBS) were acquired from Gibco (Thermo Fisher Scientific. USA). RNase- and DNase-free DEPC-treated water, RIPA lysis buffer, and a protease inhibitor cocktail were bought from Beyotime (Jiangsu, China). Olive oil (CAS: 8001-25-0) and acetone (CAS: 67-64-1) were obtained from Aladdin (Shanghai, China). The deionized water used here was prepared by using a Milli-Q system (Millipore, Boston), and all reagents were of analytical grade.

Cell Lines and Animals. The human immortalized keratinocytes HACAT (ATCCFS-0241) and mouse myoblasts C2C12 (BeNa Culture Collection, Beijing, China) were cultured at 37 °C in a humidified atmosphere with 5% CO_2 (Heraeus, Germany) in a DMEM supplemented with 10% FBS together with 100 U L^{-1} penicillin/streptomycin for less than 10 passages to sustain optimal cell viability as well as their respective inherent features. In addition, all cell lines were routinely detected for mycoplasma contamination and confirmed to be negative.

Significantly, DCs, utilized *in vitro* experiment in this paper, were referred to the bone marrow-derived DC (BMDC) subgroup, which were *ex vivo* extracted, developed, and differentiated from healthy BALB/c mice BM pre-DC populations according to a classical methodology.[35] In brief, after being separated from mice BM and the elimination of red blood cells (RBCs), the murine BM pre-DCs were maintained in RPMI 1640 complete culture medium (comprising of RPMI 1640, 10% FBS, 100 U mL^{-1} penicillin/streptomycin) containing 20 ng mL^{-1} murine recombinant cytokines GM-CSF as well as 10 ng mL^{-1} IL-4 for 7 days, and the loosely adherent cells harvested on day 7 were regarded as the immature BMDCs. Notably, to optimize the differentiation medium, the culture medium was refreshed with fresh 1640 complete medium moderately supplemented with functional cytokines IL-4 and GM-CSF every other day, and the purity of $CD11c^+$ cells (the acknowledged or prominent marker of DCs) was appraised by flow cytometry (ACEA NovoCyteTM) as a guarantee of the uniformity among batches.

Moreover, to harvest the splenic lymphocyte (SPLC) suspension, murine spleen from healthy BALB/c mouse was cautiously ground and was further filtrated though a 70 μm sterile cell strainer, and the splenic cell populations were disposed with ice-cold erythrocyte lysis buffer for removing RBCs and were subsequently purified through magnetic microbead isolation (via $CD3^+$ negative enrichment selection kit) to acquire naive $CD3^+$ T cell populations if necessary. To be worthy of attention, the complete 1640 medium (containing 10 mM NEAA, 1 mM sodium pyruvate, 2 ng·mL^{-1} IL-7, 10 ng mL^{-1} IL-250 mM, 55 μM β-mercaptoethanol, and 2 mM L-glutamine) was employed to provide optimized development and proliferation media for T cells instead of other splenic immune populations.

Male 8−10-week-old BALB/c mice (Slaccas Experimental Animal Co., Ltd. Shanghai, China) were canonically bred and maintained under pathogen-free conditions. In addition, the BALB/c mice were housed in a standard and controlled laboratory environment at 23 °C ± 3 °C in the 12 h light/dark cycle (9 a.m.−9 p.m. lights on and 9 p.m.−9 a.m. lights off) and were grouped randomly, and the relative humidity was kept from 40 to 60%. Furthermore, all experimental procedures were conducted according to the protocols approved by the Institutional Animal Care and Use Committee of Zhejiang University.

Preparation, Characterization, and Cytotoxicity of NEs. Catastrophic phase inversion together with consecutive probe-type sonication methods was exploited to yield cationic NEs, including vitamin E-incorporated NE (V-NE) and DV-NE. In brief, the oil phase was composed of PC, vitamin E, and MCT in a 2:1:1 weight ratio, together dissolved in an ethanol-based solvent. DOTAP was incorporated into this oil phase to confer cationic properties. Besides, to be worthy of attention, the oil-soluble compound DEX was necessarily added into the oil phase to fabricate DV-NE as well as PDV-NE before the nanoscale emulsion preparation. Sequentially, under the vortex-based vigorous stirring, DNase- and RNase-free DEPC-treated water, which worked as the aqueous phase, was dropwise dropped into the targeted oil phase (with or without DEX) to generate primary oil-in-water (O/W) NEs (i.e., V-NE and DV-NE). Subsequently, the V-NE and DV-NE formulations were fabricated after the primary emulsions were respectively probe sonicated (40% power, 3 min, work 2 s, pause 3 s, 2−3 rounds) on the ice bath. Notably, the V-NE and DV-NE were filtrated through the 0.4 μm sterile filter membrane twice to remove microbes and guarantee sterility. Furthermore, the anionic double-stranded RNA adjuvant to endue DCs with pro-Th1 ability, poly(I:C) was mixed with either V-NE or DV-NE at a nitrogen/phosphate (N/P) weight ratio of 4:1. This ratio allowed for efficient adsorption of the water-soluble poly(I:C) onto the NEs, resulting in nanoparticles with optimal size and a mild positive charge. These attributes contributed to enhanced delivery stability and internalization efficiency. Besides, the complexes (i.e., PV-NE and PDV-NE, respectively) composed of nanoscale emulsions and adjuvant poly(I: C) were harvested by incubating the mentioned cationic NEs and anionic adjuvant at 37 °C for 15 min. On the other hand, poly(I:C)-loaded NE without vitamin E (P-NE) was also generated in the similar approach as PV-NE. In

https://doi.org/10.1021/acsnano.4c08767
ACS Nano 2025, 19, 4195−4212

addition, to measure the poly(I:C) encapsulation efficiency and loading capacity in PV-NE, we employed an ultrafiltration−centrifugation method (10000 rpm, 10 min) to separate the free and loaded poly(I: C) molecules, used ethanol (aqueous phase: ethanol = 1:10) to trigger the release of surface-absorbed poly(I:C) from PV-NE, and detected the ultraviolet absorption OD value of free and loaded poly(I:C) in 270 nm. The poly(I:C) encapsulation efficiency in PV-NE was 98.63%, and the loading capacity of poly(I:C) in PV-NE was 2.4%.

Time-Dependent Cellular Uptake and Intracellular Drug Release. To appraise the time-dependent cellular uptake of formulations (i.e., V-NE, DV-NE, PV-NE, and PDV-NE) in antigen-presenting cells and keratinocytes, DCs and HACAT, which were both preseeded in 24-well dish with 60−80% confluence, were incubated with the mentioned four nanoscale emulsions, whose hydrophobic core were noncovalently labeled by fluorescent dye DID, for 2, 4, 8, 12, 18, and 24 h, respectively. Subsequently, the DCs and HACAT, which had already internalized a certain amount of fluorescent emulsions, were dyed with Hoechst 33342 (10 μg/mL, 37 °C, 20 min) to visualize the nucleus. The indicated cells were washed twice with 37 °C phosphate buffer saline and were postfixed with 4% formaldehyde (room temperature, 10 min) afterward. The representative fluorescence images were captured with an inverted and high-resolution fluorescence microscope (AIR, Nikon, Japan) under a constant laser intensity at appointed time points. Moreover, the acquired images were further analyzed by ImageJ to obtain semiquantitative fluorescence intensity of DID-positive DCs and HACAT.

To visualize the intracellular drug-release behavior of PV-NE within a 12 h period, we utilized hydrophilic and anionic ICG dye (green, 25 μg/mL) as a model drug to mimic surface-adsorbed poly(I:C) release, hydrophobic DID dye (red, 25 μg/mL) to label the NEs' core, and oil-soluble DIO dye (green, 25 μg/mL) as a surrogate for internally encapsulated cargoes (e.g., DEX mimics and vitamin E). A high-resolution fluorescence microscope (AIR, Nikon, Japan) captured sequential images at 2, 6, and 12 h. The absence of complete overlap between red and green fluorescence signals within DCs signified drug release.

Dosage Optimization of PV-NE. DCs generated *ex vivo*, which were seeded in a 12-well plate (with 500 μL complete 1640 culture media) and reached a confluence of 70−80%, were incubated with OVA (1 mg/mL) together with PV-NE at different doses (0, 1, 10, 20, 30, 50 ug/mL poly(I: C) in PV-NE) for 24 h, while the OVA (1 mg/mL) plus potent adjuvant LPS (1 μg/mL)-treated DCs were utilized as positive control. Subsequently, the respective culture supernatant was acquired, and the cell lysate supernatant was collected and mixed with the corresponding culture supernatant, if necessary. Then the concentrations of IFN-α and IL-12 were analyzed by ELISA kits as described in the manufacturer's detailed instructions.

Besides, to examine whether PV-NE could display augmented DC maturation competence compared to free poly(I:C), 10 μg/mL poly(I:C) in PV-NE or 10 μg/mL free poly(I: C) was used to stimulate immature DCs for 24 h in the presence of the antigen OVA (1 mg/mL). Then, the indicated DCs were harvested to detect their immunological features by flow cytometric measurement (ACEA NovoCyteTM). In brief, the DCs treated with diverse strategies were harvested and equably suspended in 100 μL of cold phosphate buffer saline respectively and were dyed with APC-conjugated anti-CD11c antibody, PE-conjugated anti-MHC II I-A/I-E, and FITC-conjugated anti-CD80 according to the manufacturer's detailed instructions. Data were further treated with the FlowJo V10 software. Meanwhile, the content of Th1-activated cytokines IFN-α and IL-12 in the respective culture supernatant was measured by ELISA kits.

***In Vitro* DC Activation.** To assess the immunological function of the indicated strategies (including the formulation type and the order of administration) in activating DCs *in vitro*, the immature DCs were, respectively, treated with saline (control), OVA (OVA), OVA plus DV-NE (DV-NE), OVA plus PV-NE (10 ug/mL) (PV-NE), OVA plus DV-NE (simultaneously) plus PV-NE (6 h later) (DV-NE + PV-NE), OVA plus PV-NE (simultaneously) plus DV-NE (6 h later) (PV-NE + DV-NE), OVA plus PDV-NE (PDV-NE), and OVA plus LPS (LPS) for 24 h. Then, the frequency of mature CD80$^+$ MHC II$^+$ DCs in CD11c$^+$ populations was appraised by flow cytometric measurement (ACEA NovoCyteTM) as mentioned above, and the IFN-α- and IL-12-secretion ability of grouped DCs were estimated by ELISA kits according to the manufacturer's instructions.

***In Vitro* T Cell Proliferation and Differentiation.** The T cell populations separated from murine spleens were cocultured with disparate agent-treated DCs (including saline, OVA, OVA + DV-NE, OVA + PV-NE, OVA + DV-NE + PV-NE, OVA + PV-NE + DV-NE, OVA + PDV-NE, and OVA + LPS) at the ratio of 20:1 for 72 h. Notably, OVA was added together with the LPS or NEs (when the single NE was used). When there existed two types of NEs, the second NE was added into the culture medium 6 h after the first NE was added. Subsequently, T cells, the nonadherent cell populations, were collected and separated to evaluate the proliferation index via the CCK-8 assay as described in the manufacturer's instructions. In addition, the intracellular along with extracellular (in culture supernatant) concentrations of Th1 production IFN-γ and Th2 cytokine IL-4 were quantified by corresponding commercial ELISA kits according to the manufacturer's instructions.

Biodistribution of Nanoscale Emulsions. For visualized track of PV-NE and PDV-NE *in vivo*, the oil-soluble fluorescent dye DIR, excited by NIR light, was utilized to prelabel the PV-NE and PDV-NE. When mice were smeared with a 1% DNCB solution (the mixed dissolvent: acetone/florence oil = 2:1 (v/v)) on the naked dorsal skin every 2 days for 1 week and then were stimulated by 0.5% DNCB for another 1 week (twice per week), the AD-bearing mice were randomly divided into two groups and were topically applied with DIR-premarked PV-NE or PDV-NE, respectively. 24 h later, mice were sacrificed, and the skin retention and permeation efficiency of the fluorescent NEs and the biodistribution in the skin and other major visceral organs (heart, liver, spleen, lung, and kidney) of the AD-bearing hosts were observed. In addition, the colocalization of AD skin-infiltrating CD11c$^+$ DCs with the DIR-NEs was further assessed via the immunofluorescence methods 24 h postadministration.

***In Vivo* Therapeutic Strategies to Alleviate AD Symptoms.** *Topical Administration of NEs in AD-Suffering Mice.* To test and validate the AD-alleviating curative effect of topically applied PV-NE, the DNCB-based AD-bearing BALB/c mouse model was built, by the 1 week 1% DNCB solution stimulation (every 2 days) and then 2-week 0.5% DNCB solution smearing (every 4 days). The AD-bearing BALB/c mice were randomly divided into six groups (n = 5 biologically independent animals in each group) and then received the topical application of different preparations (including DEX cream on the market, PV-NE, DEX (first) plus PV-NE (6 h later), PV-NE (first) plus DEX (6 h later), and PDV-NE) on the naked dorsal skin every day. The used dose of PV-NE was 0.6 mg/kg (referred to the equivalent concentration of poly(I:C), and each milliliter of the PV-NE solution contained 150 μg of poly(I:C) together with 1.35 mg of vitamin E), and the used volume was 100 μL. Notably, we monitored the scratching behavior, severity, and the body weight of the grouped mice every 2 days until the termination of the experiment. The severity score and the digital photos were both used to record the severity of the AD, and the severity score was evaluated according to the signs and symptoms of AD: (1) dryness, (2) excoriation/erosion, (3) erythema/hemorrhage, (4) scratch, and (5) lichenification (0: no symptom; 0.5−1: mild; 1.5−2.5: moderate; 3−3.5: severe; 4−5: extremely severe). At the terminal day (30 days later), all the mice were euthanized, and the inflamed skins were collected to analyze the AD recovery or severity. The concentration of the serum biochemical indicator (IgE), as well as the type 2 cytokine (IL-4) content and the TSLP content in the skin foci, was detected by the commercial ELISA kit. Besides, considering CD11c serving as the most important and recognized marker of DCs, we detected the relative frequency of inflammatory skin-infiltrating CD11c$^+$ DCs by immunohistochemical staining. The relative amounts of inflammation-infiltrating CD4$^+$ IL-4$^+$ Th2 and CD4$^+$ IFN-γ^+ Th1 within the DNCB-stimulated skin regions were measured by immunofluorescence staining. The hematoxylin−

https://doi.org/10.1021/acsnano.4c08767
ACS Nano 2025, 19, 4195−4212

eosin (H&E) staining was used to reflect the biotoxicity of the indicated formulations.

Topical Administration of Formulations in AD Mice under Recurrent Attacks. First, the BALB/c mice were stimulated with a 1% DNCB solution (the mixed dissolvent: acetone/florence oil = 2:1 (v/v)) thrice within 1 week, and then the mice were randomly grouped into six groups, which were respectively treated with different formulations (including commercial DEX cream, PV-NE, DEX plus PV-NE (6 h later), PV-NE plus DEX (6 h later), and PDV-NE) every day within consecutive 3 weeks. To simulate the recurrent manifestation of AD, the mice accepted 0.5% DNCB stimulation during the whole treatment (n = 6 biologically independent mice in each group). The dosage of PV-NE was 0.6 mg/kg (referred to the equivalent concentration of poly(I:C)). The severity score, digital photos, and body weight of the mice were obtained every 2 days until the end of the experiment. 21 days later, the IgE content in the serum and the concentration of TLSP, IL-4 together with IFN-γ of inflamed skin, were respectively assessed via the commercial ELISA kits. The H&E staining and immunohistochemical staining of CD11c along with the immunofluorescence staining (of $CD4^+$ $IL\text{-}4^+$ Th2 and $CD4^+$ IFN-γ^+ Th1) were used to appraise the inflammatory properties of the skin with AD lesion after being treated by the indicated strategies.

Estimating the Synergistic Effect of ROS Scavenger and Adjuvant. The male BALB/c mice were first stimulated with 1% DNCB for 1 week, which were further randomly divided into three groups (control, P-NE, and PV-NE, respectively). And then the grouped mice were topically administrated with indicated treatments (i.e., P-NE and PV-NE) every day in the consecutive 25 days, and the 0.5% DNCB was used to smear on the back area of the mice to imitate the recurrent feature of AD. The body weight, severity score, and digital images were recorded every 2 days until day 25 (the termination of the experiment). At the end of the experiment, the ROS content, the IL-4 concentration, the IFN-γ content along with the TSLP content within the inflamed skin, and the IgE content in the serum were detected according to the manufacturer's instructions. Furthermore, the H&E staining and immunohistochemical staining of CD11c were employed to estimate the pathology structure and DC infiltration of the AD lesional region.

Statistical Analysis. Data were represented as mean ± standard error. Comparisons between two or several groups were analyzed using unpaired student's t tests. All presented data are representative. The fluorescent images were viewed, processed, and analyzed by ImageJ. To conduct the best possible analysis of results from fluorescent images, all experiments were performed independently at least three times, and those experiments yielded the same results. All statistical analyses were carried out by GraphPad Prism version 8.4 software (San Diego, CA), with a value of $P < 0.05$ considered to be statistically significant.

ASSOCIATED CONTENT

Data Availability Statement

The raw/processed data required to reproduce these findings can be shared by the authors upon request.

Supporting Information

The Supporting Information is available free of charge at https://pubs.acs.org/doi/10.1021/acsnano.4c08767.

AD features with skin inflammation and intense itch; fabrication and characterization of NEs; PV-NE effectively induces DCs into pro-Th1 type compared to free poly(I:C); schematic illustration of how DCs initiate and stimulate naïve T cells into Th1 and Th2 cells; PV-NE endues DCs with pro-Th1 immunological ability; treatment strategies and corresponding effects in DNCB-induced AD-bearing mice model; biosafety of indicated formulations in DNCB-induced AD-bearing mice model; quantitative intensity of CD11c expression in AD skin from DNCB-induced AD-bearing mice model; the therapeutic strategies and anti-AD effect in mice facing recurrent AD attacks; biosafety and SLOs of indicated formulations in AD mice with persistent DNCB stimulation; quantitative intensity of CD11c expression in AD locus of mice with persistent DNCB stimulation; cytokine concentration in AD mice with persistent DNCB stimulation; TEM images to reflect morphologies of nanoscale emulsion P-NE; combined ROS elimination and adjuvant regulation arouse synergistically anti-AD effect; quantitative intensity of CD11c expression in AD mice lesion; biosafety of indicated treatments in AD mice (PDF)

AUTHOR INFORMATION

Corresponding Authors

Ping Huang − *Center for Clinical Pharmacy, Cancer Center, Department of Pharmacy, Zhejiang Provincial People's Hospital (Affiliated People's Hospital), Hangzhou Medical College, Hangzhou, Zhejiang 310014, P.R. China; Zhejiang Provincial Clinical Research Center for Head & Neck Cancer, Hangzhou 310014, China; Zhejiang Key Laboratory of Precision Medicine Research on Head & Neck Cancer, Hangzhou 310014, China*; Phone: 086-0571-87666666; Email: huangping@hmc.edu.cn

Lihua Luo − *College of Pharmaceutical Sciences, Zhejiang University, Hangzhou, Zhejiang 310058, P. R. China; Zhejiang-California International NanoSystems Institute, Hangzhou, Zhejiang 310058, P. R. China*; Phone: 086-0571-88981651; Email: luolihua@zju.edu.cn

Jian You − *College of Pharmaceutical Sciences, Zhejiang University, Hangzhou, Zhejiang 310058, P. R. China; Zhejiang-California International NanoSystems Institute, Hangzhou, Zhejiang 310058, P. R. China; Jinhua Institute of Zhejiang University, Jinhua, Zhejiang 321299, P. R. China*; orcid.org/0000-0002-7114-6299; Phone: 086-0571-88981651; Email: youjiandoc@zju.edu.cn

Authors

Yichao Lu − *College of Pharmaceutical Sciences, Zhejiang University, Hangzhou, Zhejiang 310058, P. R. China; Center for Clinical Pharmacy, Cancer Center, Department of Pharmacy, Zhejiang Provincial People's Hospital (Affiliated People's Hospital), Hangzhou Medical College, Hangzhou, Zhejiang 310014, P.R. China; Zhejiang Provincial Clinical Research Center for Head & Neck Cancer, Hangzhou 310014, China; Zhejiang Key Laboratory of Precision Medicine Research on Head & Neck Cancer, Hangzhou 310014, China*

Xinyu Shan − *College of Pharmaceutical Sciences, Zhejiang University, Hangzhou, Zhejiang 310058, P. R. China*

Jiaxin Huang − *College of Pharmaceutical Sciences, Zhejiang University, Hangzhou, Zhejiang 310058, P. R. China*

Huanli Zhou − *College of Pharmaceutical Sciences, Zhejiang University, Hangzhou, Zhejiang 310058, P. R. China*

Ying Zhu − *College of Pharmaceutical Sciences, Zhejiang University, Hangzhou, Zhejiang 310058, P. R. China*

Sijie Wang − *College of Pharmaceutical Sciences, Zhejiang University, Hangzhou, Zhejiang 310058, P. R. China*

Zhenyu Luo − *College of Pharmaceutical Sciences, Zhejiang University, Hangzhou, Zhejiang 310058, P. R. China*

Xu Liu − *College of Pharmaceutical Sciences, Zhejiang University, Hangzhou, Zhejiang 310058, P. R. China*

https://doi.org/10.1021/acsnano.4c08767
ACS Nano 2025, 19, 4195−4212

Xuemeng Guo − *College of Pharmaceutical Sciences, Zhejiang University, Hangzhou, Zhejiang 310058, P. R. China*
Yingying Shi − *College of Pharmaceutical Sciences, Zhejiang University, Hangzhou, Zhejiang 310058, P. R. China*
Yilong Hu − *College of Pharmaceutical Sciences, Zhejiang University, Hangzhou, Zhejiang 310058, P. R. China*
Huihui Liu − *College of Pharmaceutical Sciences, Zhejiang University, Hangzhou, Zhejiang 310058, P. R. China*
Junlei Zhang − *College of Pharmaceutical Sciences, Zhejiang University, Hangzhou, Zhejiang 310058, P. R. China*

Complete contact information is available at: https://pubs.acs.org/10.1021/acsnano.4c08767

Author Contributions

#Y.L., X.S., and J.H. are first authors.

Notes

The authors declare no competing financial interest.

ACKNOWLEDGMENTS

National Nature Science Foundation of China (82003667 and 82273862), Zhejiang Province Public Welfare Project LGF22H300003, State Key Laboratory for Diagnosis & Treatment of Infectious Diseases (zz202305), China National Postdoctoral Program for Innovative Talents (BX20230321), and the National Key R&D Program of China (2023YFC340200).

REFERENCES

(1) Langan, S. M.; Irvine, A. D.; Weidinger, S. Atopic dermatitis. *Lancet* **2020**, *396* (10247), 345−360.
(2) Facheris, P.; Jeffery, J.; Del Duca, E.; Guttman-Yassky, E. The translational revolution in atopic dermatitis: the paradigm shift from pathogenesis to treatment. *Cellular & Molecular Immunology* **2023**, *20* (5), 448−474.
(3) Weidinger, S.; Beck, L. A.; Bieber, T.; Kabashima, K.; Irvine, A. D. Atopic dermatitis. *Nat. Rev. Disease Primers* **2018**, *4* (1), 1.
(4) Bieber, T. Atopic dermatitis: an expanding therapeutic pipeline for a complex disease. *Nat. Rev. Drug Discovery* **2022**, *21* (1), 21−40.
(5) Klaeschen, A. S.; Nümm, T. J.; Herrmann, N.; Leib, N.; Maintz, L.; Sakai, T.; Wenzel, J.; Bieber, T. JAK1/2 inhibition impairs the development and function of inflammatory dendritic epidermal cells in atopic dermatitis. *J. Allergy Clinical Immunol.* **2021**, *147* (6), 2202−2212.
(6) Bangert, C.; Rindler, K.; Krausgruber, T.; Alkon, N.; Thaler, F. M.; Kurz, H.; Ayub, T.; Demirtas, D.; Fortelny, N.; Vorstandlechner, V.; Bauer, W. M.; Quint, T.; Mildner, M.; Jonak, C.; Elbe-Bürger, A.; Griss, J.; Bock, C.; Brunner, P. M. Persistence of mature dendritic cells, TH2A, and Tc2 cells characterize clinically resolved atopic dermatitis under IL-4Rα blockade. *Sci. Immunol.* **2021**, *6* (55), No. eabe2749.
(7) Yosipovitch, G.; Mollanazar, N.; Ständer, S.; Kwatra, S. G.; Kim, B. S.; Laws, E.; Mannent, L. P.; Amin, N.; Akinlade, B.; Staudinger, H. W.; Patel, N.; Yancopoulos, G. D.; Weinreich, D. M.; Wang, S.; Shi, G.; Bansal, A.; O'Malley, J. T. Dupilumab in patients with prurigo nodularis: two randomized, double-blind, placebo-controlled phase 3 trials. *Nature Medicine* **2023**, *29* (5), 1180−1190.
(8) Li, H.; Zhang, Z.; Zhang, H.; Guo, Y.; Yao, Z. Update on the Pathogenesis and Therapy of Atopic Dermatitis. *Clinical Reviews in Allergy & Immunology* **2021**, *61* (3), 324−338.
(9) Biadsee, A.; Payne, S.; Sowerby, L. J. Can we make biologic therapy more affordable? *International Forum of Allergy & Rhinology* **2022**, *12* (9), 1087−1088.
(10) Kapsenberg, M. L. Dendritic-cell control of pathogen-driven T-cell polarization. *Nature Reviews Immunology* **2003**, *3* (12), 984−993.
(11) Field, A. K.; Tytell, A. A.; Lampson, G. P.; Hilleman, M. R. Inducers of interferon and host resistance. II. Multistranded synthetic polynucleotide complexes. *Proc. Natl. Acad. Sci. U. S. A.* **1967**, *58* (3), 1004−1010.
(12) Hokey, D. A.; Larregina, A. T.; Erdos, G.; Watkins, S. C.; Falo, L. D., Jr Tumor Cell Loaded Type-1 Polarized Dendritic Cells Induce Th1-Mediated Tumor Immunity. *Cancer Res.* **2005**, *65* (21), 10059−10067.
(13) Liu, T.; Xiao, B.; Xiang, F.; Tan, J.; Chen, Z.; Zhang, X.; Wu, C.; Mao, Z.; Luo, G.; Chen, X.; Deng, J. Ultrasmall copper-based nanoparticles for reactive oxygen species scavenging and alleviation of inflammation related diseases. *Nat. Commun.* **2020**, *11* (1), 2788.
(14) Jia, Y.; Hu, J.; An, K.; Zhao, Q.; Dang, Y.; Liu, H.; Wei, Z.; Geng, S.; Xu, F. Hydrogel dressing integrating FAK inhibition and ROS scavenging for mechano-chemical treatment of atopic dermatitis. *Nat. Commun.* **2023**, *14* (1), 2478.
(15) Ribeiro, A. M.; Estevinho, B. N.; Rocha, F. The progress and application of vitamin E encapsulation − A review. *Food Hydrocolloids* **2021**, *121*, No. 106998.
(16) Lu, Y.; Shi, Y.; Luo, Z.; Guo, X.; Jiang, M.; Li, X.; Zhang, J.; Zhu, C.; Yin, H.; Qin, B.; Liu, X.; Huang, J.; Du, Y.; Luo, L.; You, J. Reactivation of dysfunctional dendritic cells by a stress-relieving nanosystem resets anti-tumor immune landscape. *Nano Today* **2022**, *43*, No. 101416.
(17) Hertweck, A.; Vila de Mucha, M.; Barber, P. R.; Dagil, R.; Porter, H.; Ramos, A.; Lord, G. M.; Jenner, R. G. The TH1 cell lineage-determining transcription factor T-bet suppresses TH2 gene expression by redistributing GATA3 away from TH2 genes. *Nucleic Acids Res.* **2022**, *50* (8), 4557−4573.
(18) Novak, N. An update on the role of human dendritic cells in patients with atopic dermatitis. *Journal of Allergy and Clinical Immunology* **2012**, *129* (4), 879−886.
(19) Lu, Y.; Shi, Y.; You, J. Strategy and clinical application of up-regulating cross presentation by DCs in anti-tumor therapy. *J. Controlled Release* **2022**, *341*, 184−205.
(20) Lu, Y.; Shi, Y.; Liu, Y.; Luo, Z.; Zhang, J.; Jiang, M.; Li, X.; Liu, X.; Guo, X.; Qin, B.; Yin, H.; Du, Y.; Qiu, Y.; Lou, Y.; Guan, G.; Luo, L.; You, J. A therapeutic DC vaccine with maintained immunological activity exhibits robust anti-tumor efficacy. *J. Controlled Release* **2022**, *349*, 254−268.
(21) Lu, Y.; You, J. Strategy and application of manipulating DCs chemotaxis in disease treatment and vaccine design. *Biomedicine & Pharmacotherapy* **2023**, *161*, No. 114457.
(22) van Panhuys, N.; Klauschen, F.; Germain, R. N. T-Cell-Receptor-Dependent Signal Intensity Dominantly Controls CD4+ T Cell Polarization In Vivo. *Immunity* **2014**, *41* (1), 63−74.
(23) Wculek, S. K.; Cueto, F. J.; Mujal, A. M.; Melero, I.; Krummel, M. F.; Sancho, D. Dendritic cells in cancer immunology and immunotherapy. *Nat. Rev. Immunol* **2020**, *20* (1), 7−24.
(24) Longhi, M. P.; Trumpfheller, C.; Idoyaga, J.; Caskey, M.; Matos, I.; Kluger, C.; Salazar, A. M.; Colonna, M.; Steinman, R. M. Dendritic cells require a systemic type I interferon response to mature and induce CD4+ Th1 immunity with poly IC as adjuvant. *Journal of Experimental Medicine* **2009**, *206* (7), 1589−1602.
(25) de Jong, E. C.; Smits, H. H.; Kapsenberg, M. L. Dendritic cell-mediated T cell polarization. *Springer Seminars in Immunopathology* **2005**, *26* (3), 289−307.
(26) Brossart, P.; Kotthoff, P. Dexamethasone Promotes Fungal Infection By Inhibition of APC Activation with Beta-Glucans Via STAT-3 and NF-κb. *Blood* **2016**, *128* (22), 3710−3710.
(27) Kim, S.-H.; Moon, J.-H.; Jeong, S.-U.; Jung, H.-H.; Park, C.-S.; Hwang, B. Y.; Lee, C.-K. Induction of antigen-specific immune tolerance using biodegradable nanoparticles containing antigen and dexamethasone. *International journal of nanomedicine* **2019**, *14*, 5229−5242.
(28) Dainichi, T.; Kitoh, A.; Otsuka, A.; Nakajima, S.; Nomura, T.; Kaplan, D. H.; Kabashima, K. The epithelial immune microenvironment (EIME) in atopic dermatitis and psoriasis. *Nature Immunology* **2018**, *19* (12), 1286−1298.

(29) Song, H.-Y.; Kim, W. S.; Mushtaq, S.; Park, J. M.; Choi, S.-H.; Cho, J.-W.; Lim, S.-T.; Byun, E.-B. A novel chrysin derivative produced by gamma irradiation attenuates 2,4-dinitrochlorobenzene-induced atopic dermatitis-like skin lesions in Balb/c mice. *Food Chem. Toxicol.* **2019**, *128*, 223−232.
(30) Oetjen, L. K.; Mack, M. R.; Feng, J.; Whelan, T. M.; Niu, H.; Guo, C. J.; Chen, S.; Trier, A. M.; Xu, A. Z.; Tripathi, S. V.; Luo, J.; Gao, X.; Yang, L.; Hamilton, S. L.; Wang, P. L.; Brestoff, J. R.; Council, M. L.; Brasington, R.; Schaffer, A.; Brombacher, F.; Hsieh, C. S.; Gereau, R. W.; Miller, M. J.; Chen, Z. F.; Hu, H.; Davidson, S.; Liu, Q.; Kim, B. S. Sensory Neurons Co-opt Classical Immune Signaling Pathways to Mediate Chronic Itch. *Cell* **2017**, *171* (1), 217−228.
(31) Wilson, S. R.; Thé, L.; Batia, L. M.; Beattie, K.; Katibah, G. E.; McClain, S. P.; Pellegrino, M.; Estandian, D. M.; Bautista, D. M. The Epithelial Cell-Derived Atopic Dermatitis Cytokine TSLP Activates Neurons to Induce Itch. *Cell* **2013**, *155* (2), 285−295.
(32) Schuler, C. F.; Billi, A. C.; Maverakis, E.; Tsoi, L. C.; Gudjonsson, J. E. Novel insights into atopic dermatitis. *Journal of Allergy and Clinical Immunology* **2023**, *151* (5), 1145−1154.
(33) Gen, R.; Akbay, E.; Sezer, K. Cushing Syndrome Caused by Topical Corticosteroid: A Case Report. *American Journal of the Medical Sciences* **2007**, *333* (3), 173−174.
(34) Igarashi, A.; Yuasa, A.; Yonemoto, N.; Kamei, K.; LoPresti, M.; Murofushi, T.; Ikeda, S. A Systematic Literature Review of Economic Evaluations and Cost Studies of the Treatment of Psoriasis, Atopic Dermatitis, and Chronic Urticaria. *Dermatology and Therapy* **2022**, *12* (8), 1729−1751.
(35) Son, Y. I.; Egawa, S. I.; Tatsumi, T.; Redlinger, R. E.; Kalinski, P.; Kanto, T. A novel bulk-culture method for generating mature dendritic cells from mouse bone marrow cells. *Journal of Immunological Methods* **2002**, *262* (1−2), 145−157.

https://doi.org/10.1021/acsnano.4c08767
ACS Nano 2025, 19, 4195−4212